AD NUMBER

AD875070

LIMITATION CHANGES

TO:

Approved for public release; distribution is unlimited. Document partially illegible.

FROM:

Distribution authorized to U.S. Gov't. agencies and their contractors; Critical Technology; AUG 1970. Other requests shall be referred to Air Force Technical Applications Center, VSC, Alexandria, VA 22313. This document contains export-controlled technical data.

AUTHORITY

usaf ltr, 25 jan 1972

AFTAC Project No. VELA/T/0701/B/ASD

TFO AND UBO LONG-PERIOD ARRAY DATA ANALYSIS

Technical Report No. 8

SEISMIC ARRAY PROCESSING TECHNIQUES

Prepared by

Gary D. McNeely

Stanley J. Laster, Project Scientist
Frank H. Binder, Program Manager
Area Code 214, 238-6521

TEXAS INSTRUMENTS INCORPORATED
Services Group
P. O. Box 5621
Dallas, Texas 75222

Contract No. F33657-70-C-0100
Amount of Contract: $339,052
Beginning 15 July 1969
Ending 14 July 1970

Prepared for

AIR FORCE TECHNICAL APPLICATIONS CENTER
Washington, D. C. 20333

Sponsored by

ADVANCED RESEARCH PROJECTS AGENCY
Nuclear Monitoring Research Office
ARPA Order No. 624
ARPA Program Code No. 9F10

12 August 1970

Acknowledgment: This research was supported by the Advanced Research Projects Agency, Nuclear Monitoring Research Office, under Project VELA-UNIFORM, and accomplished under the technical direction of the Air Force Technical Applications Center under Contract No. F33657-70-C-0100.

AFTAC Project No. VELA/T/0701/B/ASD

TFO AND UBO LONG-PERIOD ARRAY DATA ANALYSIS

Technical Report No. 8

SEISMIC ARRAY PROCESSING TECHNIQUES

Prepared by

Gary D. McNeely

Stanley J. Laster, Project Scientist
Frank H. Binder, Program Manager
Area Code 214, 238-6521

TEXAS INSTRUMENTS INCORPORATED
Services Group
P. O. Box 5621
Dallas, Texas 75222

Contract No. F33657-70-C-0100
Amount of Contract: $339,052
Beginning 15 July 1969
Ending 14 July 1970

Prepared for

AIR FORCE TECHNICAL APPLICATIONS CENTER
Washington, D. C. 20333

Sponsored by

ADVANCED RESEARCH PROJECTS AGENCY
Nuclear Monitoring Research Office
ARPA Order No. 624
ARPA Program Code No. 9F10

12 August 1970

Acknowledgment: This research was supported by the Advanced Research Projects Agency, Nuclear Monitoring Research Office, under Project VELA-UNIFORM, and accomplished under the technical direction of the Air Force Technical Applications Center under Contract No. F33657-70-C-0100.

This document is subject to special export controls and each transmittal to foreign governments or foreign nationals may be made only with prior approval of Chief, AFTAC.

Qualified users may request copies of this document from:

Defense Documentation Center
Cameron Station
Alexandria, Virginia 22314

TABLE OF CONTENTS

LIST OF ILLUSTRATIONS

LIST OF ILLUSTRATIONS (CONT'D)

LIST OF ILLUSTRATIONS (CONT'D)

LIST OF TABLES

ABSTRACT

Results of the analysis of two long-period noise samples from Tonto Forest Seismological Observatory (TFO) and three from Uinta Basin Seismological Observatory (UBO) are presented. Analysis methods include single channel power density spectra, determination of multichannel coherences, and computation of two-dimensional frequency-wavenumber spectra. Results are compared to results obtained earlier from the Montana Large Aperture Seismic Array; the noise fields at the three sites are found to be generally similar. Comparison of array processing methods for the UBO and TFO data indicate that little more than 2 db noise suppression improvement above the 6-7 db obtainable by beamsteer processing can be expected from multichannel filter processing. There is some evidence of acoustically coupled low-frequency propagating noise in the TFO data.

SECTION I

INTRODUCTION AND PRINCIPAL CONCLUSIONS

This report presents the results of the analysis of two long-period noise samples from Tonto Forest Seismological Observatory (TFO) and three from Uinta Basin Seismological Observatory (UBO). Results are presented principally in terms of single channel power density spectra, two-dimensional frequency-wavenumber power density spectra, and multichannel coherences. Also presented are comparisons between some of the characteristics of the noise fields at TFO and UBO and the noise field at the Montana Large Aperture Seismic Array (LASA).

The following are the most significant conclusions reached:

- The long-period noise fields at TFO and UBO are basically similar to the noise field at LASA. The most significant points of similarity in the three noise fields are these:
  - Single channel power density spectra at each array show spectral peaks between 0.05-0.07 Hz and 0.11-0.14 Hz, and considerable variability in the spectra at each array below 0.05 Hz however, noise levels are generally lower at TFO and UBO.
  - The noise fields at all three arrays show relatively high coherence near the lower spectral peak (0.05-0.07 Hz).
  - Most of the propagating noise at each array appears to be fundamental Rayleigh mode energy, with some evidence of higher frequency P-wave noise appearing in quiet summer data.
- There is some evidence of acoustically coupled propagating low-frequency noise at TFO.

- A comparison of array processing methods indicates that little more than 2 db average noise reduction above the 6-7 db achievable by beamsteer processing could be expected from MCF processing of TFO and UBO data.

SECTION II

DATA PROCESSING

A. DATA RECORDING

The two TFO noise samples analyzed were selected from a series of noise samples recorded digitally from the seven element array of 3-component long-period seismometers during the period from 27 January 1969 through 3 March 1969. Quality of the recorded data was generally poor; each of the two noise samples selected, which represent the best of the data, has at least one bad channel among each set of components. There are also short segments of bad data on the generally good channels.

The first TFO noise sample begins at 1351 Z on 21 February 1969 and covers a period of 2 hours, 4 minutes. The second begins at 0250 Z on 1 March 1969 and covers a period of 1 hour, 55 minutes. The original sample period (Δt) was 0.096 sec; the data was decimated by a factor of 20 to yield a sample period of 1.92 sec and a Nyquist frequency of 0.26 Hz. Since the seismometer response has a sharp cut-off, no anti-alias filtering was necessary prior to re-sampling.

The three noise samples recorded digitally from the seven element array of 3-component long-period seismometers at UBO were obtained from Seismic Data Laboratories. Each noise sample was one hour and 15 minutes long; the dates and starting times of the three noise samples are 1225 Z, 27 July 1969; 1800 Z, 27 July 1969; and 1227 Z, 30 July 1969. The sample

period of this data is two seconds, giving a Nyquist frequency of 0.25 Hz. Data quality is similar to that of the TFO data.

B. COMPUTATION OF POWER DENSITY SPECTRA

Power density spectra were computed by the maximum entropy method[1] for each useable channel from each noise sample and were plotted. The vertical scale for each spectrum is expressed in db in terms of millimicrons squared per Hz relative to one millicron squared per Hz of ground motion power density. In the case of the TFO data, the necessary calibration information in terms of digital units per millimicron of ground motion for each channel was obtained from a digitally recorded station calibration test. The frequency employed in the test was 0.04 Hz. The information for the UBO recorded data, valid at 0.04 Hz, was supplied by Seismic Data Laboratores. No correction for instrument response at other frequencies has been made for either the UBO or TFO data.

The program which computed the single channel power density spectra also output the RMS level for each channel; this information was used along with the calibration information to arrive at tables of RMS noise levels in millimicrons for each channel.

C. FOURIER TRANSFORMATION OF THE DATA

The data were transformed from the time to the frequency domain using the fast Fourier transform algorithm. The segment length used for the Fourier transforms was 128 points for the TFO data; since the sample lengths were shorter, 64 point segments were used to transform the UBO data.

These segment lengths and the sample periods stated above give frequency increments of 0.0041 Hz and 0.0078 Hz for the TFO and UBO transforms, respectively.

The transform program was run in two versions; one employed no smoothing in the frequency domain and the other smoothed the data in the frequency domain by Hanning.[2] To compensate for the uneven weighting of the time series data introduced by Hanning in the frequency domain, overlapping gates were used in transforming the time series data - each new data segment transformed begins at the center of the last segment transformed. The short segments of bad data which occurred in each noise sample were skipped over by the transform program; also, bad channels were omitted from the computation. The transforms for all channels from each segment were multiplexed so that each output transform contained the transformed data for all good channels in the segment.

D. CROSSPOWER MATRIX GENERATION

The transforms from this program were input to a crosspower matrix generation program which computes from each input transform F(f) the crosspower matrix elements

$$\Phi_{ij}(f) = F_i^*(f)\, F_j(f)$$

at each frequency. The resulting matrices are stacked at each frequency to form a single crosspower matrix at each frequency for each noise sample. In the case of the north-south and east-west components in the first and second UBO noise samples, less than four channels were useable. Since this is too few channels to permit the calculation of satisfactory wavenumber spectra, these components were omitted from the crosspower matrix calculations for

these noise samples. Two sets of crosspower matrices were computed, one from the Hanned and one from the un-Hanned data.

E. MCF-RELATED PROCESSING

The crosspower matrices were used to compute two-dimensional frequency-wavenumber (f-k) power density spectra for each useable set of like components for each noise sample. Both conventional (beamsteer) and high resolution (maximum likelihood) spectra were computed in each case. The frequencies at which the spectra were computed for display were chosen from regions of the single channel power density spectra which showed significant peaks or troughs. Because inspection of the first set of f-k spectra computed showed very similar results for both the Hanned and un-Hanned data, only the un-Hanned data were used in the remaining data processing and in data display. Also, for similar reasons, the conventional f-k spectra plots are not presented below.

Using azimuth intervals of ten degrees and wavenumber values corresponding to the fundamental Rayleigh mode wave velocity at the chosen frequency, the f-k power density program also computed for each chosen frequency the ratio of the noise power from a single sensor to the noise power from the array processor. The computation was done for both the maximum likelihood and beamsteer processors. The Rayleigh wave velocities used were obtained from theoretical dispersion curves calculated from estimated crustal models.

The crosspower matrices were also used to obtain multiple coherences, which show the degree to which a given element can be predicted

from a linear combination of other elements of each array. The results are presented below in terms of the prediction error at each frequency where

$$\text{prediction error} = (\text{1-coherence squared})^{.5}$$

The prediction error computed is a biased estimate of the true prediction error; a correction factor[3] has been applied to each computed prediction error to compensate for this bias. The coherence between the vertical component and the two horizontal components at each instrument location and between each component at the center of the array and other like components of the array were determined and are presented along with the other results in the following section.

SECTION III

RESULTS OF DATA PROCESSING

Results of the TFO and UBO long-period data analysis are presented in chronological order below. In addition to the results of the methods of analysis described above, wave height charts for the twelve hour interval closest to the noise sample are presented.

A. FIRST TFO NOISE SAMPLE – 1351 Z, 21 FEBRUARY 1969

Single channel power density spectra for the vertical (Z), north-south (N), and east-west (E) components for the first TFO noise sample are presented in Figure III-1, along with a diagram of the array configuration. All spectra display two spectral peaks - one in the 0.05 to 0.07 Hz range and the other in the 0.11 to 0.14 Hz range. Below 0.05 Hz there is generally more power in the horizontal than in the vertical spectra. Also, the spectra fall off sharply above 0.14 Hz.

The RMS noise levels for this noise sample are given in Table III-1. The noise levels of like components at different sites vary by more than a factor of two, with LP1 being the quietest and LP6 the noisiest site. Most of this difference appears to be accounted for by differences in spectral levels below 0.05 Hz.

Plots summarizing the spatial organization of the noise sample are shown in Figure III-2. In this condensed presentation the f-k spectra for all selected frequencies for a given set of components are shown on the same plot, with only the most significant peaks from the contour plot at each frequency being displayed. In this presentation and those following which show

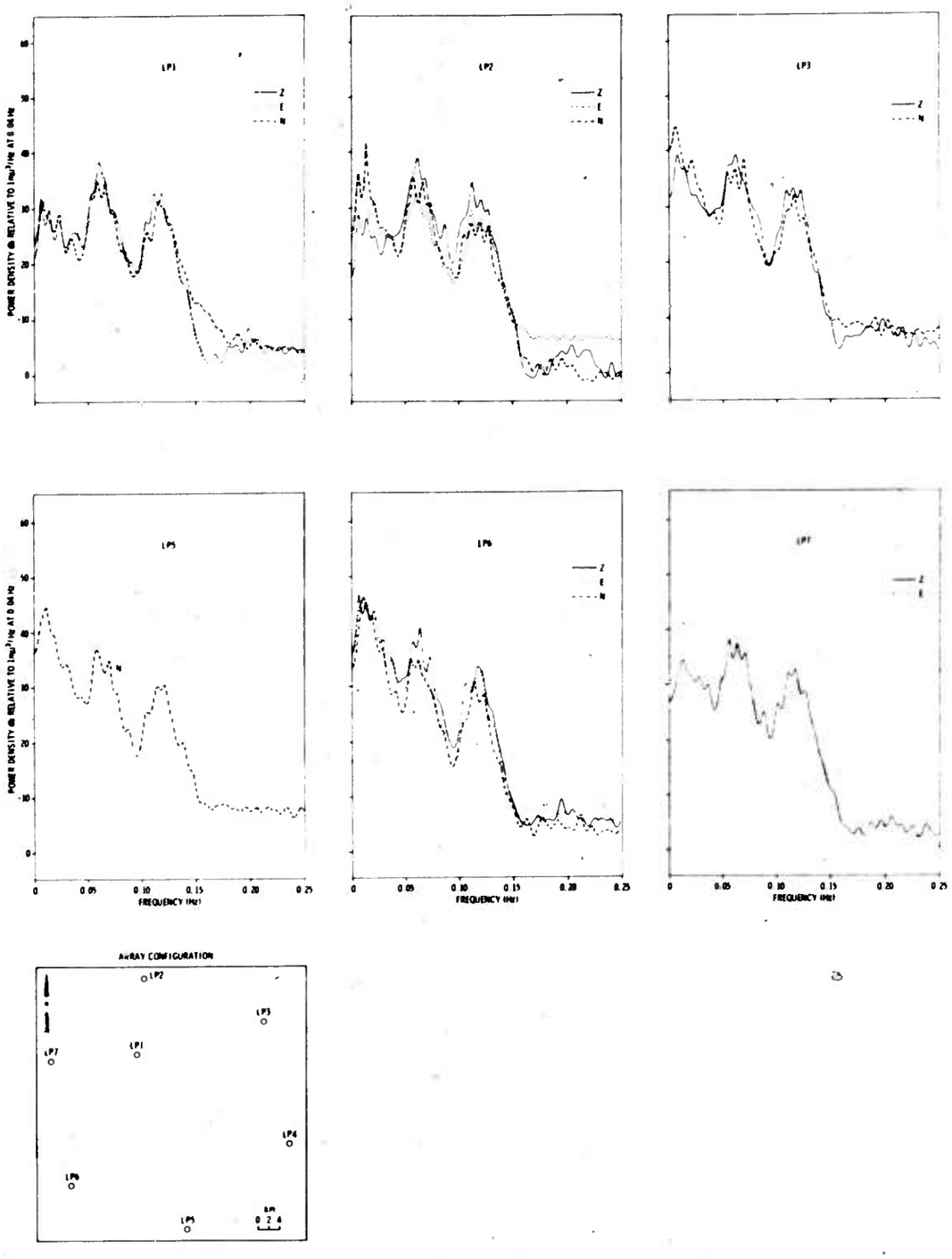

Figure III-1. Single Channel Power Density Spectra-First TFO Noise Sample

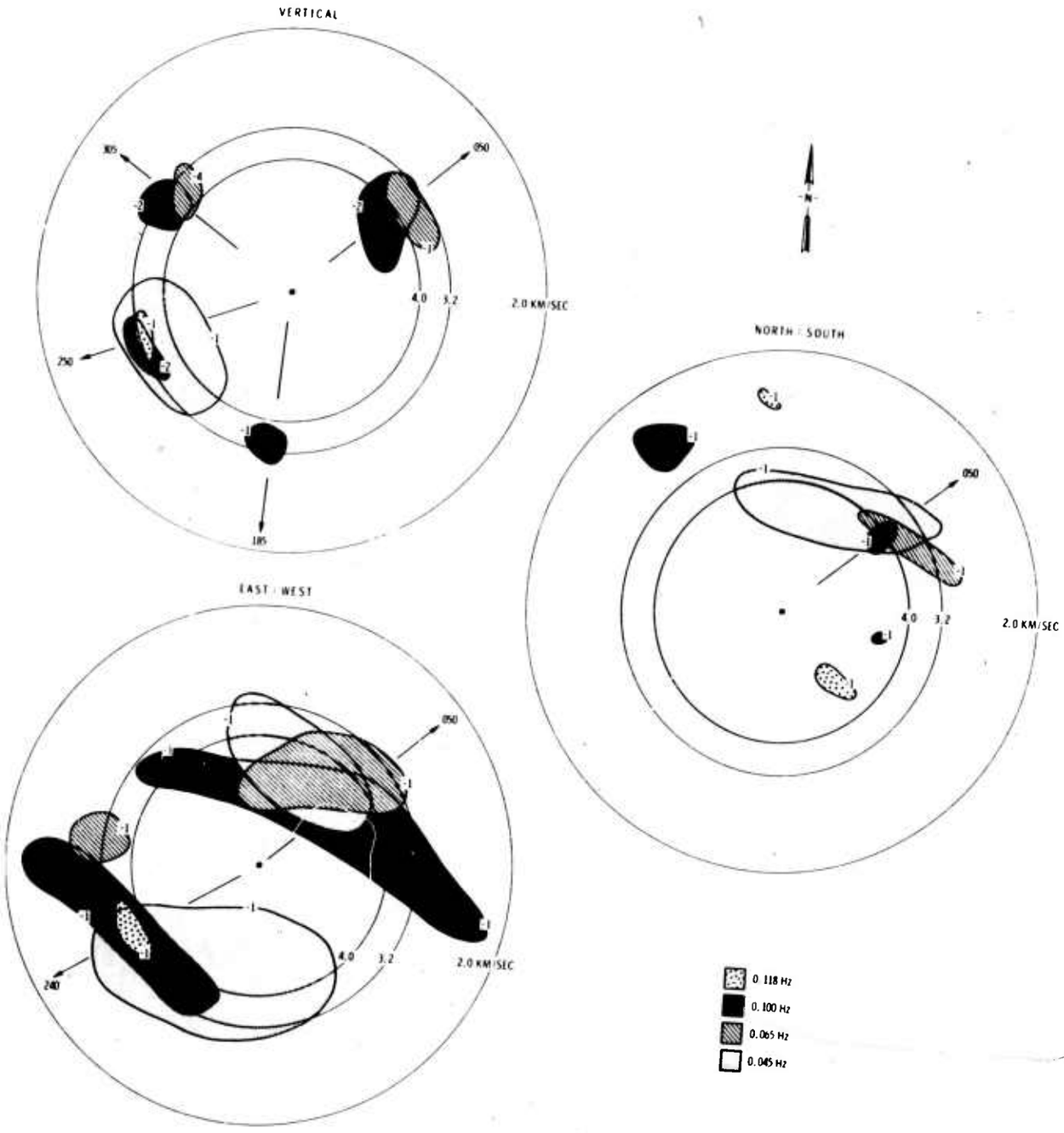

Figure III-2. Wavenumber Spectra - First TFO Noise Sample

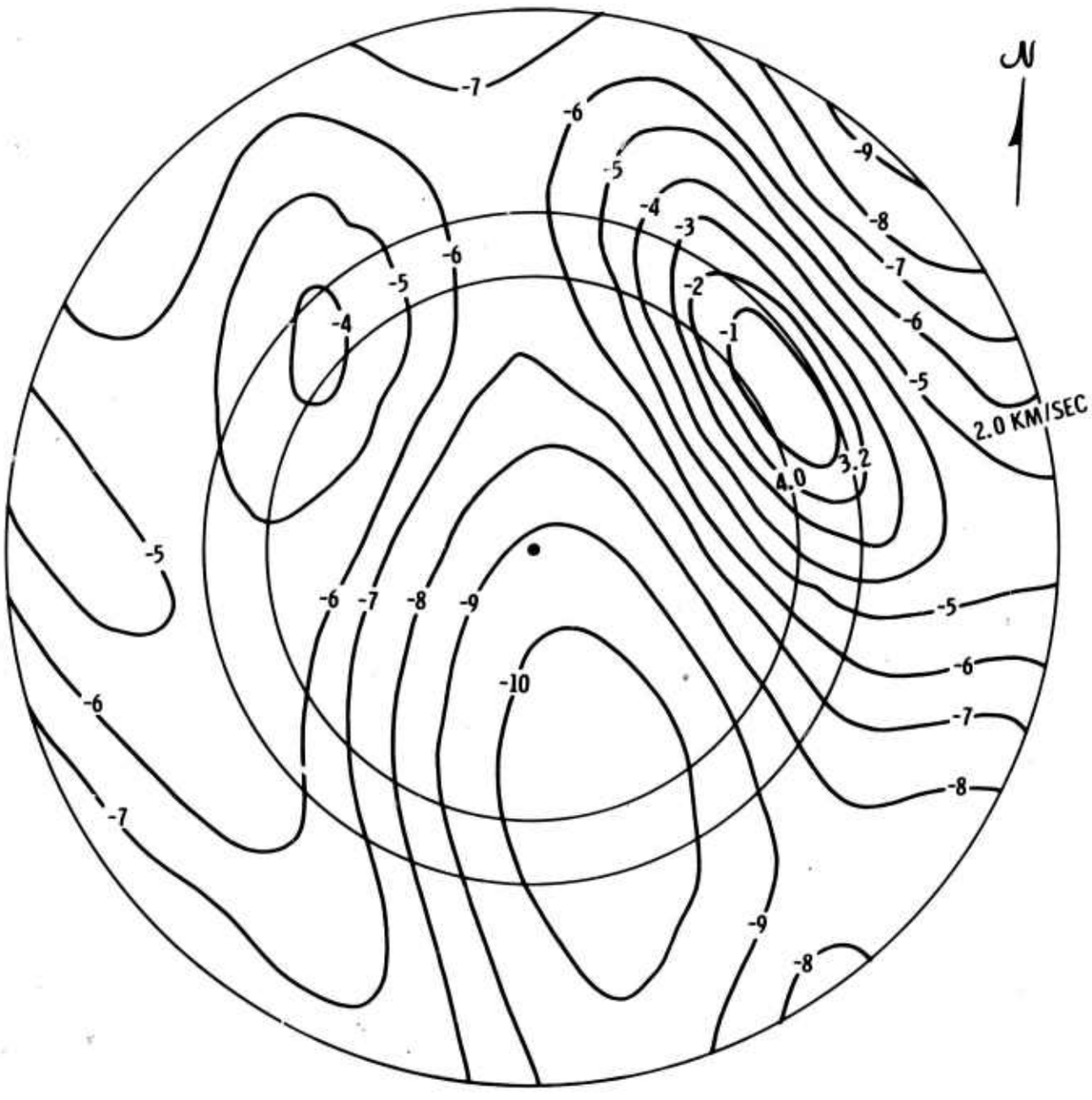

Figure III-3. Vertical Component Wavenumber Spectrum at 0.065 Hz-First TFO Noise Sample

Figure III-4. Waveheight Contour Chart at 1200 Z, 21 February 1969

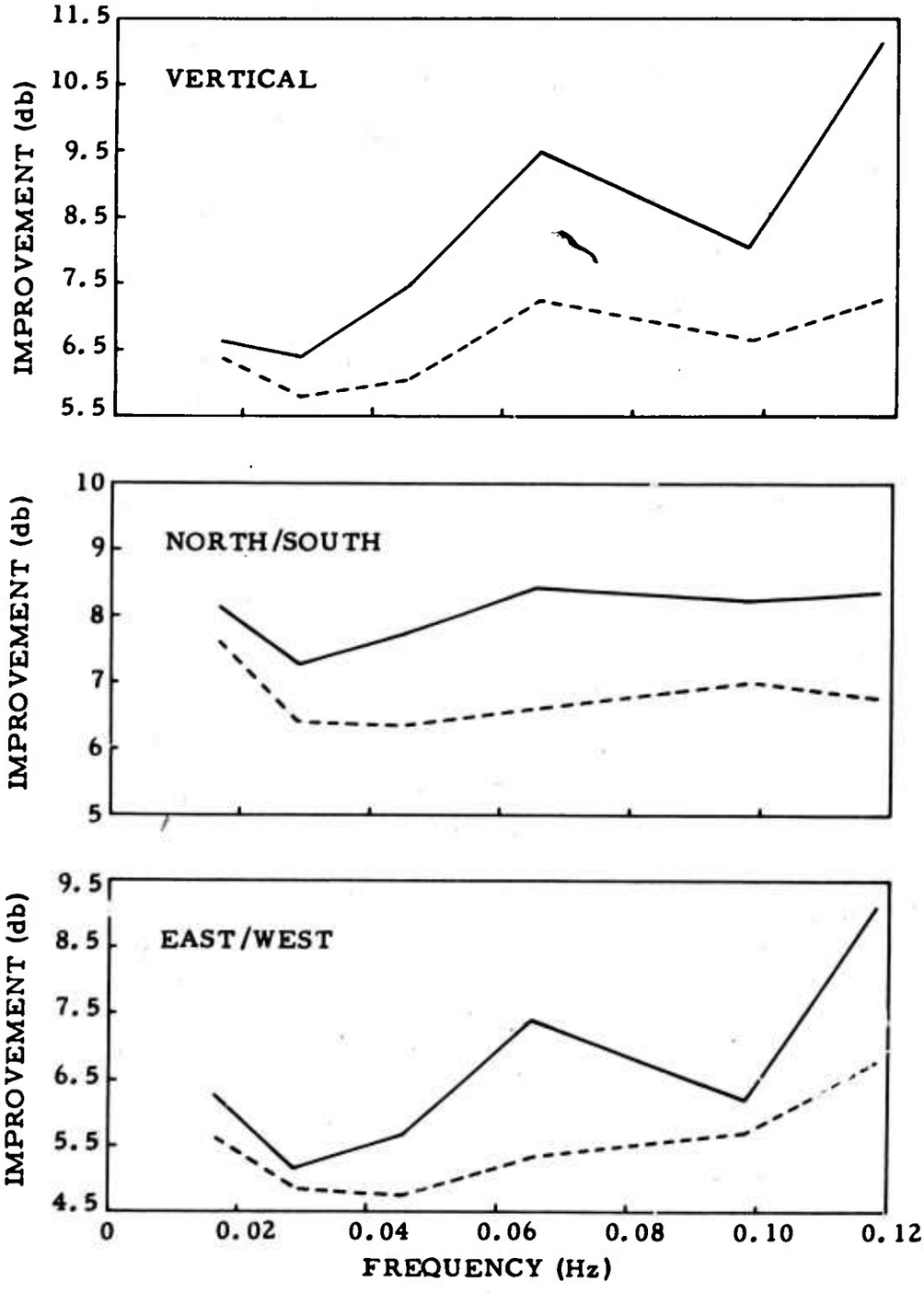

Figure III-5. Noise Rejection Improvement vs Frequency-First TFO Noise Sample

more than one frequency, the db levels indicated for each peak are given with respect to the highest power level in the f-k spectrum for that frequency, and not with respect to the db levels shown for the peaks at other frequencies.

To compare this form of presentation with an example of the f-k plots from which it was derived, the 0.065 Hz f-k contour plot for the vertical components of this noise sample is shown in Figure III-3.

The peaks in Figure III-2 show that most of the noise peaks fall within the Rayleigh-wave velocity band ($\approx$ 3.2 - 4.0 km/sec) and that most of this energy comes from azimuths near 050^{o} - 070^{o} and 240^{o} - 250^{o}. Nearly all the energy in the single channel spectral peak at 0.065 Hz comes from 050^{o} - 070^{o}.

Figure III-4 is the wave height contour chart for 1200 Z, 21 February 1969, on which are shown azimuth lines from TFO at 10^{o} increments. The strongest wave activity appears to be along the Atlantic Coast at an azimuth of approximately 65^{o}. This wave activity appears to be the source of the propagating noise coming from the northeast in this noise sample. The energy from 240^{o} - 250^{o} does not appear to be related to wave activity.

In Figure III-5 the ratios in db of the noise power from a single sensor to the noise power from the array processor are shown as a function of frequency. The ratios, which for each frequency had been calculated as a function of azimuth at wavenumber magnitudes corresponding to the Rayleigh wave velocity, have been averaged to obtain a single value for each frequency. The results here show that the improvement of the array processors over a

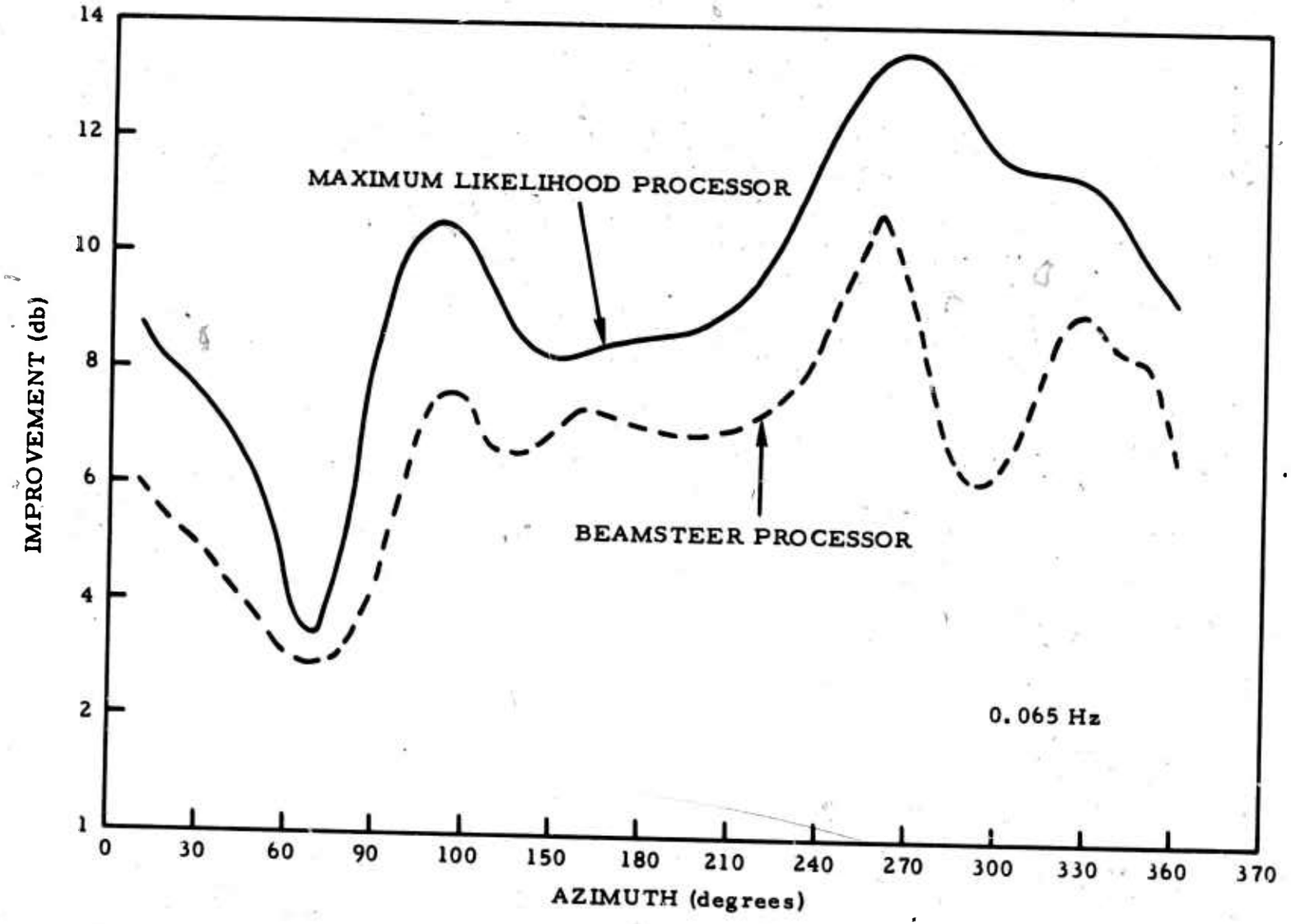

Figure III-6. Noise Rejection Improvement vs Azimuth at 0.065 Hz-First TFO Noise Sample

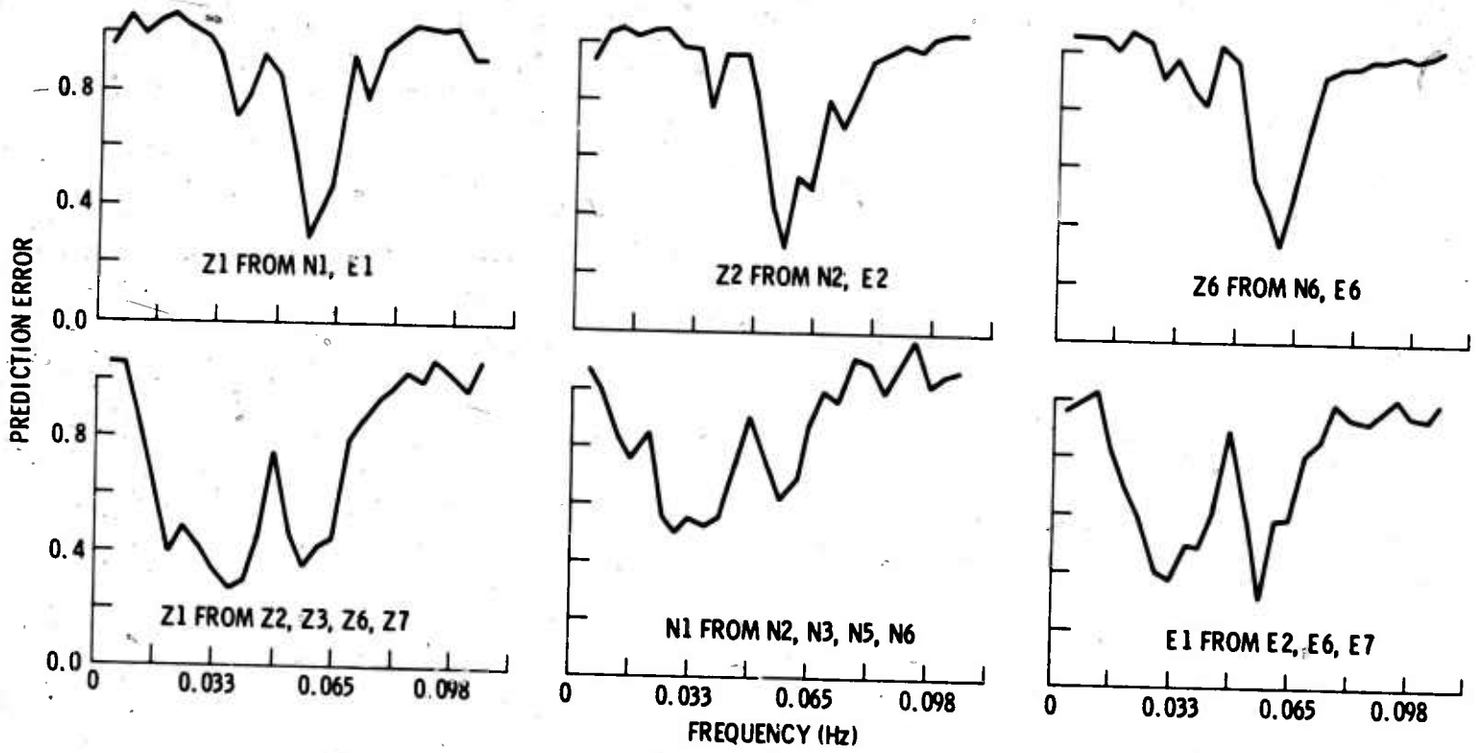

Figure III-7. Multiple Coherences-First TFO Noise Sample

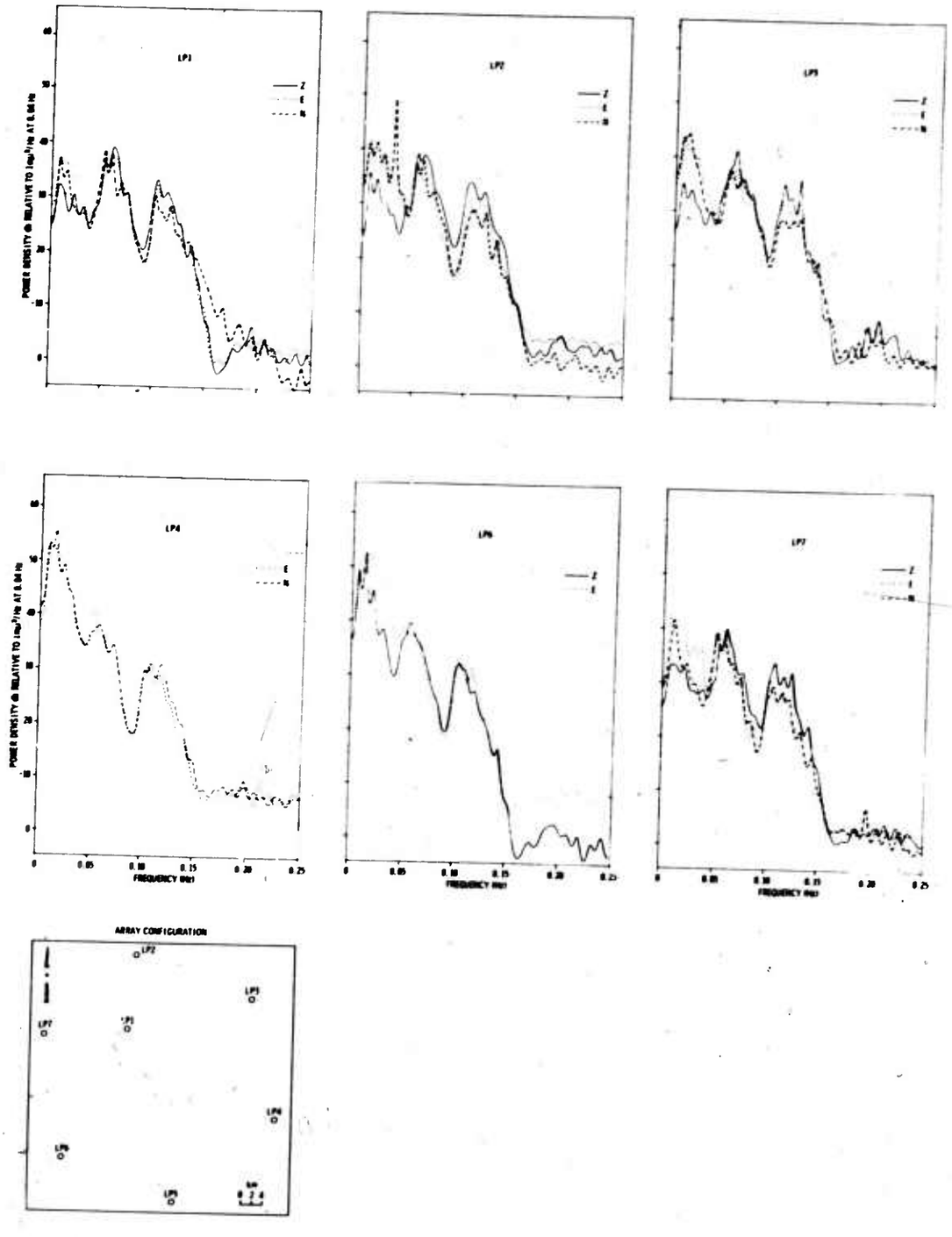

Figure III-8. Single Channel Power Density Spectra-Second TFO Noise Sample

single sensor is best at frequencies corresponding to the peaks in the single channel power density spectra. In the case of the vertical components, the beamsteer processor shows an average improvement of about 6.5 db over a single sensor and the maximum likelihood processor an improvement of about 8.5 db. For the other components also the maximum likelihood processor does only about 2 db better than the beamsteer processor on the average.

To show an example of the variability of this ratio with azimuth, the ratios for both processors are presented in Figure III-6 as a function of azimuth at 0.065 Hz. The vertical component data were used for this plot. The improvement of the maximum likelihood processor varies more than 10 db for different azimuths.

The multiple coherences computed from the first TFO noise sample are shown in Figure III-7. There is significant coherence between the vertical and the two horizontal components at the same site near 0.057 Hz, which is in the region of the lower single-channel power spectral density peak. The coherence between each center component and other like components is significant at this frequency, 0.057 Hz, and also in the region of 0.037 Hz.

B. SECOND TFO NOISE SAMPLE – 0240 Z, 1 MARCH 1969

Single channel power density spectra from the second TFO noise sample are presented in Figure III-8. These spectra are very similar to those of the first noise sample: there are spectral peaks in the ranges from 0.05 - 0.07 Hz and from 0.11 - 0.14 Hz; there is substantially more power in the horizontal than in the vertical component spectra below 0.05 Hz; and the spectra fall off above 0.14 Hz.

Table III-1

R. M. S. NOISE LEVELS FOR TFO
NOISE SAMPLES (in mμ)

Location	LPZ	LPN	LPE
	First Sample		
LP1	24.3	20.9	22.1
LP2	26.2	25.2	21.2
LP3	35.8	44.4	*
LP4	*	*	*
LP5	*	43.3	*
LP6	56.6	47.7	54.4
LP7	28.1	*	40.3
	Second Sample		
LP1	27.3	25.6	29.5
LP2	32.3	55.5	35.7
LP3	34.3	45.5	43.5
LP4	*	113.2	94.9
LP5	*	*	*
LP6	70.2	*	110.3
LP7	31.1	32.2	39.7

* – Indicates bad channels

The RMS levels for this noise sample are given in Table III-1. Again, most of the differences in RMS levels among different sites for this noise sample occur below 0.05 Hz. This observation also holds true for differences between spectra of the same site for the two noise samples.

The condenced f-k spectra for this noise sample are shown in Figure III-9. The energy falls generally within the Rayleigh wave band. Most of the energy comes from azimuths centered near 75°, 235°, and 300°.

The wave height contour chart for 0000 Z, 1 March 1969 is shown in Figure III-10. There is strong wave activity along the New England Coast at azimuths near 075°; this is probably the source of the Rayleigh wave energy coming from this azimuth in the f-k spectra. There is a region of high wave activity along an azimuth of 300° from TFO, but the area is not near a coastline. The energy appearing at azimuths near 235° in the f-k spectra seems to be unrelated to wave activity.

The noise power ratios as a function of frequency are shown in Figure III-11. In the case of the vertical components, the improvement in noise rejection over a single channel averages about 8.6 db for the maximum likelihood processor and 6.5 db for the beamsteer processor. This average difference of approximately 2 db between the processors also holds for the other two sets of components.

Multiple coherences computed from the second TFO noise sample are shown in Figure III-12.

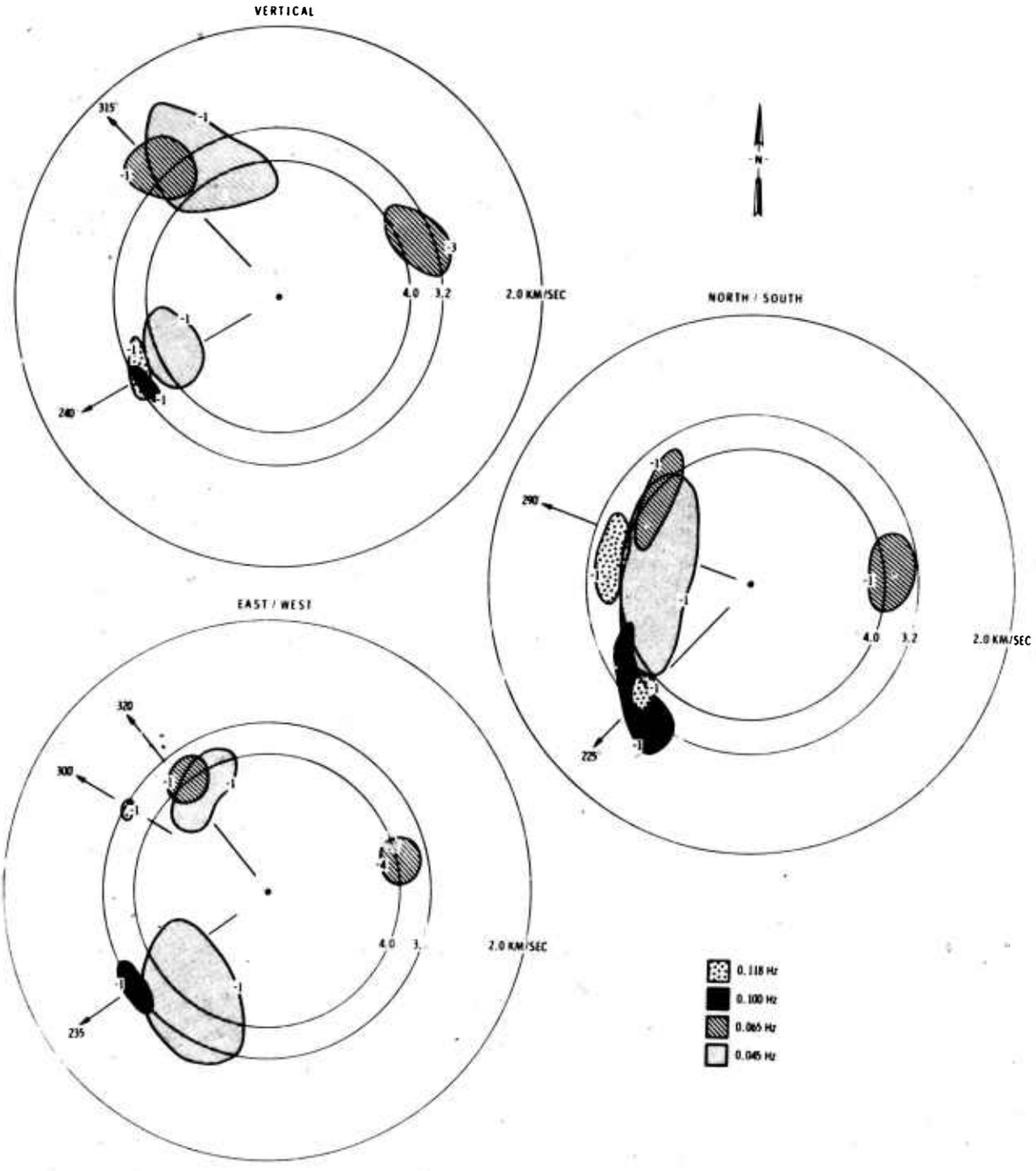

Figure III-9. Wavenumber Spectra-Second TFO Noise Sample

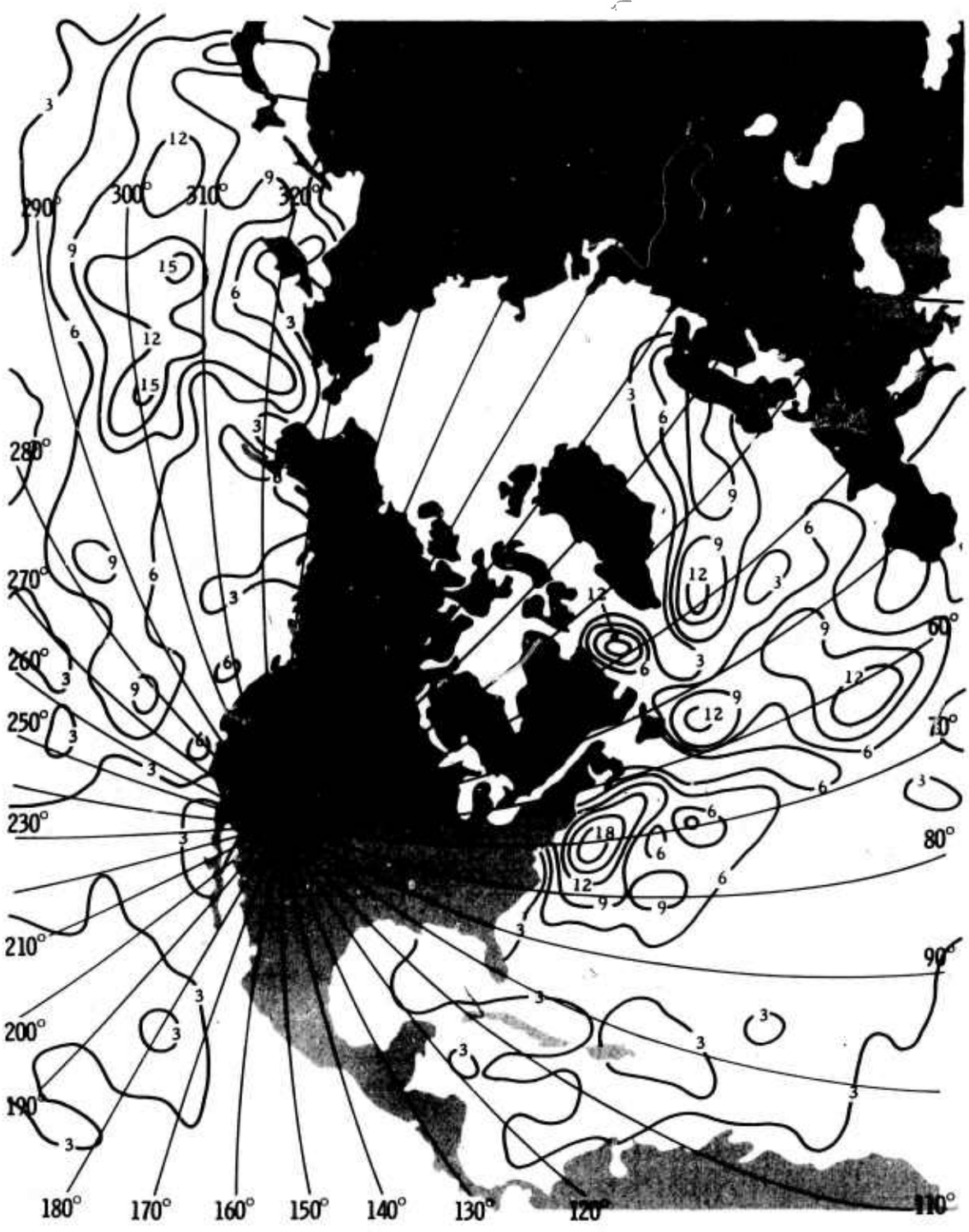

Figure III-10. Wavehight Contour Chart at 0000 Z, 1 March 1969

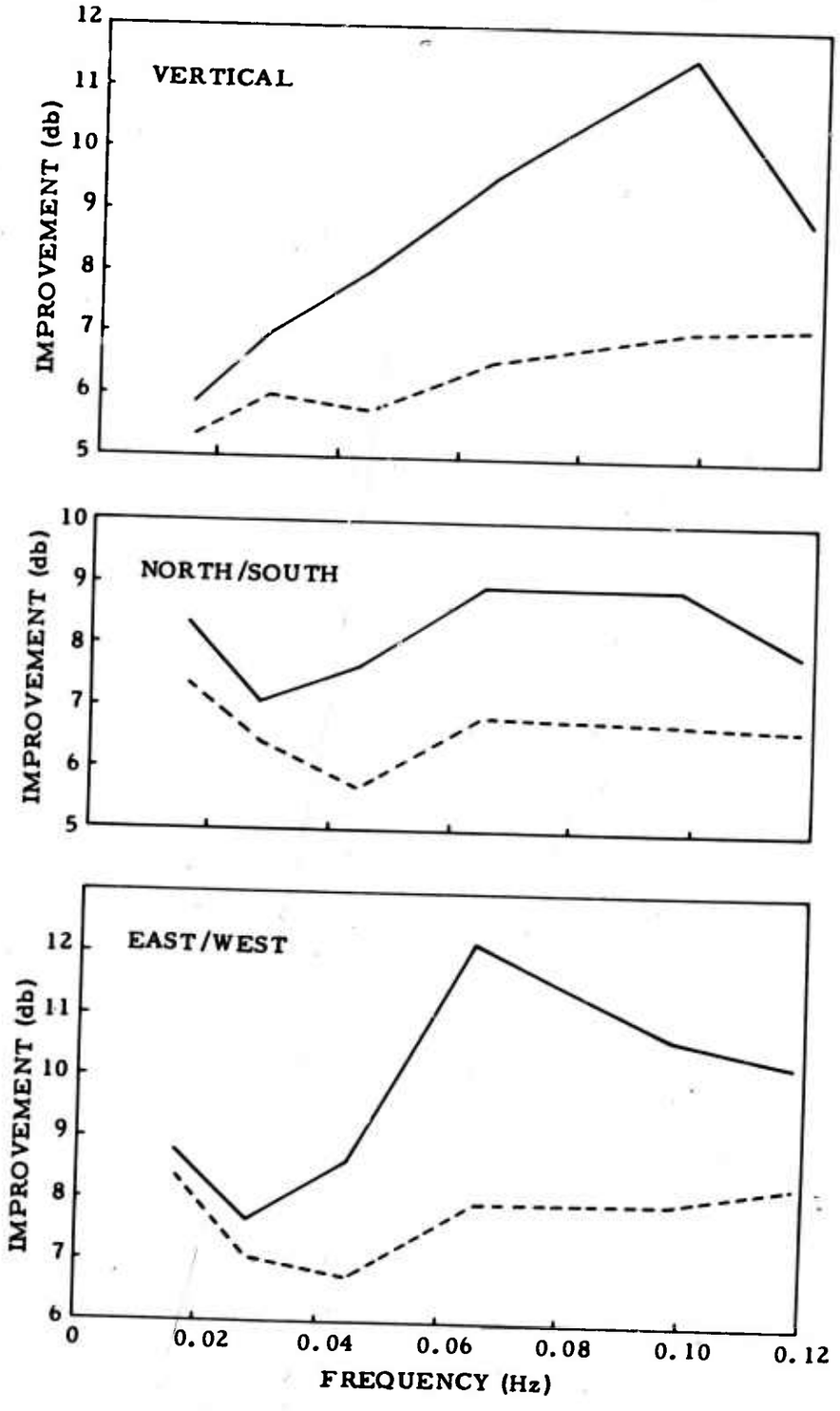

Figure III-11. Noise Rejection Improvement vs Frequency-Second TFO Noise Sample

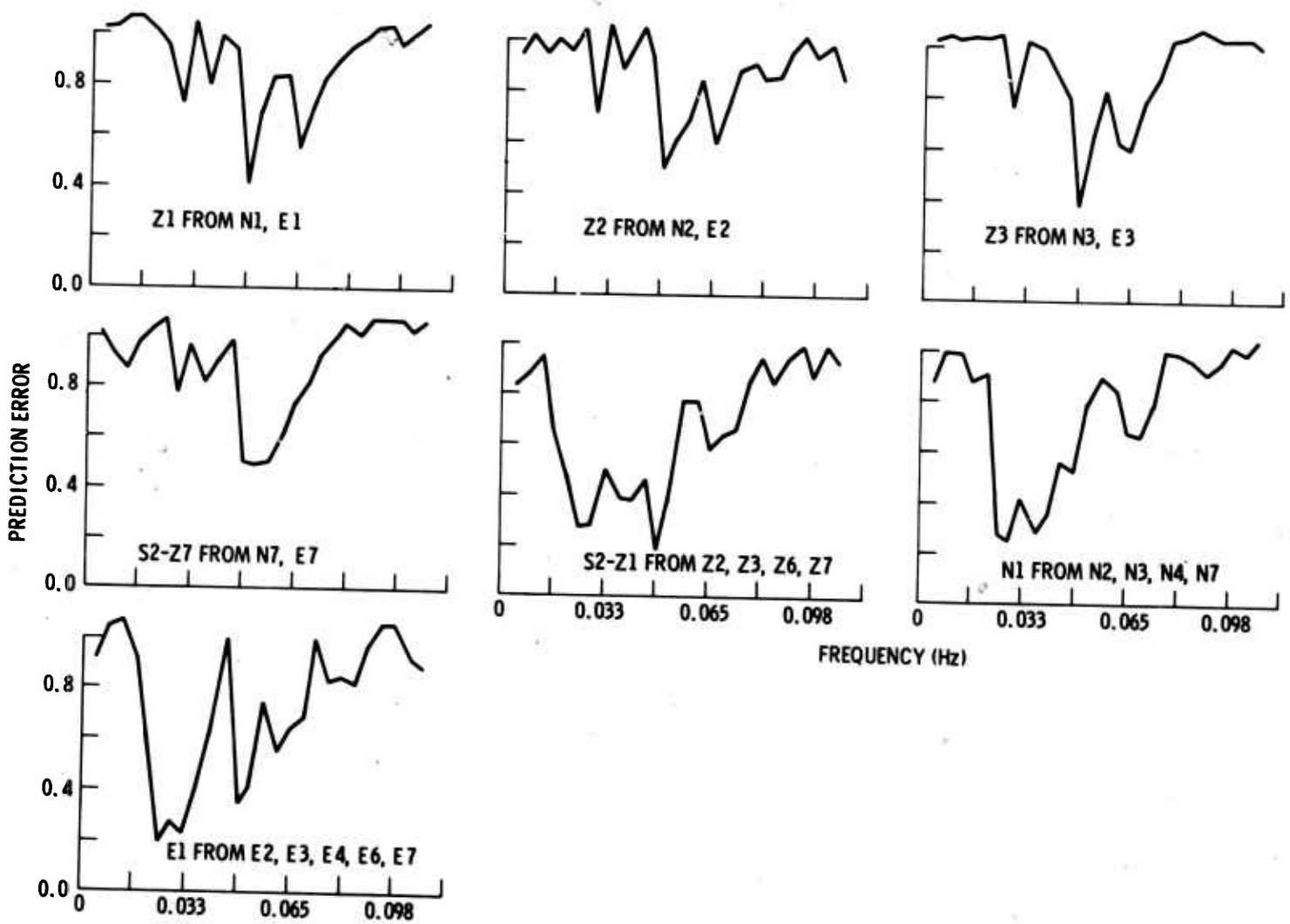

Figure III-12. Multiple Coherences-Second TFO Noise Sample

These coherences are roughly similar to those of the first noise sample; however, the region of most coherence occurs at lower frequencies in this noise sample.

C. FIRST UBO NOISE SAMPLE – 1225 Z, 27 JULY 1969

Single channel power density spectra computed from the first UBO noise sample are shown in Figure III-13, along with a diagram of the UBO array configuration. These summer noise spectra exhibit many of the features observed in the TFO winter noise. The most significant features are again the two spectral peaks, the first in the 0.05 - 0.07 Hz range and the second in the 0.11 - 0.14 Hz range. Also, the horizontal channel noise levels are significantly higher than the verticals in the region below 0.05 Hz. Here, however, the spectra of most of the channels are nearly white except for the regions of the two noise peaks. The near whiteness of the spectral levels outside the regions of the peaks, indicates that the data is system noise limited. The levels of the two spectral peaks average several db lower for the UBO noise samples than for the TFO samples.

The RMS noise levels for the first UBO noise sample are given in Table III-2. The noise levels show a somewhat smaller site-to-site variation than the TFO RMS noise levels. The overall noise levels are significantly lower than those at TFO; this is very possibly due to the fact that the UBO noise samples were recorded in the summer.

The condensed f-k spectra for this noise sample are shown in Figure III-14. All the significant propagating energy occurs in the range of fundamental Rayleigh mode velocities, and most comes from azimuths near 230^{o}.

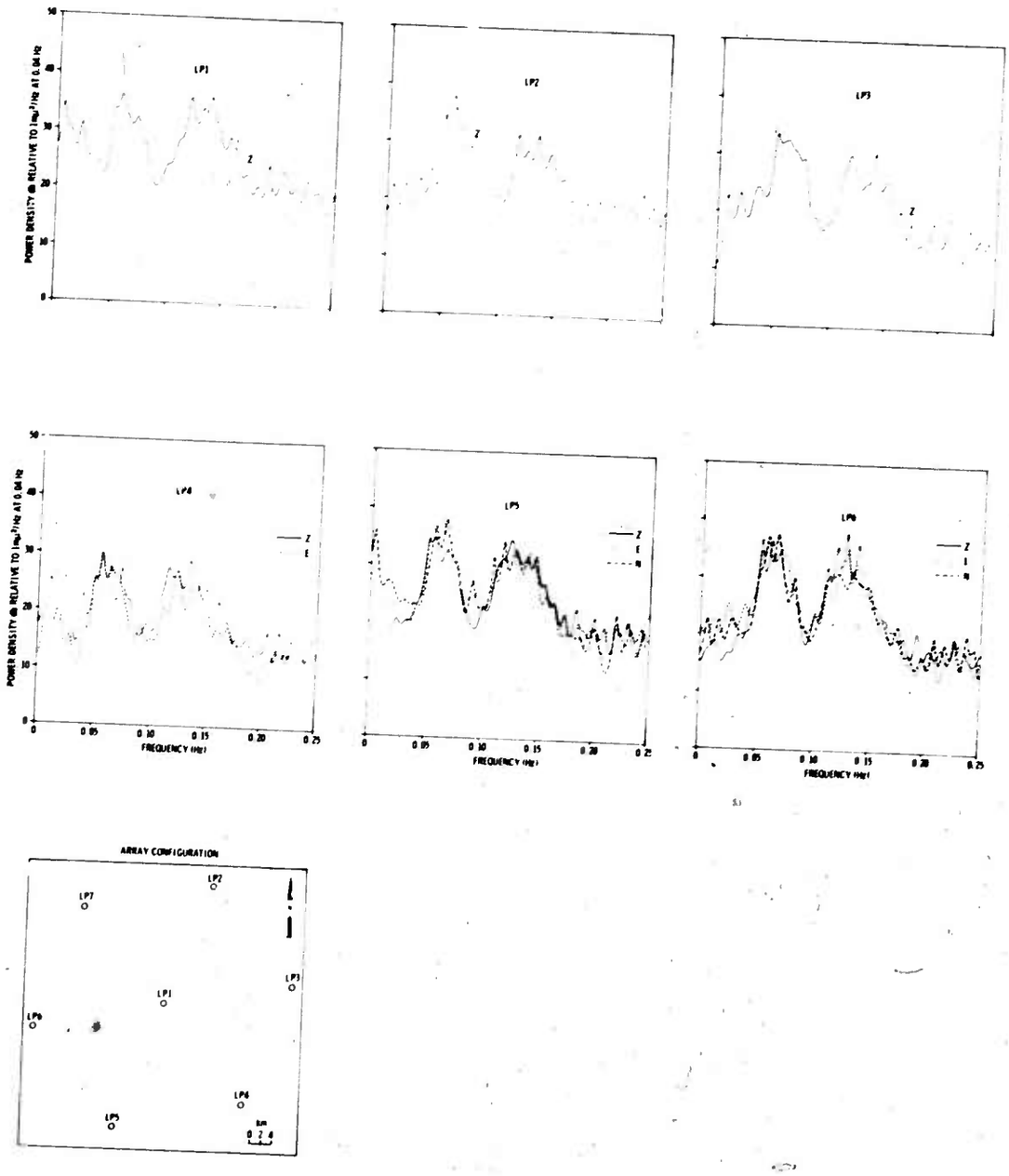

Figure III-13. Single Channel Power Density Spectra-First UBO Noise Sample

Table III-2

R. M. S. NOISE LEVELS FOR UBO NOISE SAMPLES (in mμ)

Location	LPZ	LPN	LPE
	First Sample		
LP1	28.4	*	*
LP2	19.6	*	*
LP3	17.8	*	*
LP4	*	*	10.3
LP5	23.4	26.3	26.3
LP6	26.1	23.1	25.6
LP7	*	*	*
	Second Sample		
LP1	28.8	*	*
LP2	19.1	*	*
LP3	19.0	*	*
LP4	*	*	*
LP5	22.9	*	*
LP6	24.3	*	25.4
LP7	*	*	*
	Third Sample		
LP1	30.1	*	*
LP2	19.7	23.0	19.4
LP3	17.7	*	18.5
LP4	*	*	10.3
LP5	22.5	24.7	26.4
LP6	22.5	20.1	*
LP7	24.6	20.3	22.7

* – Indicates bad channels

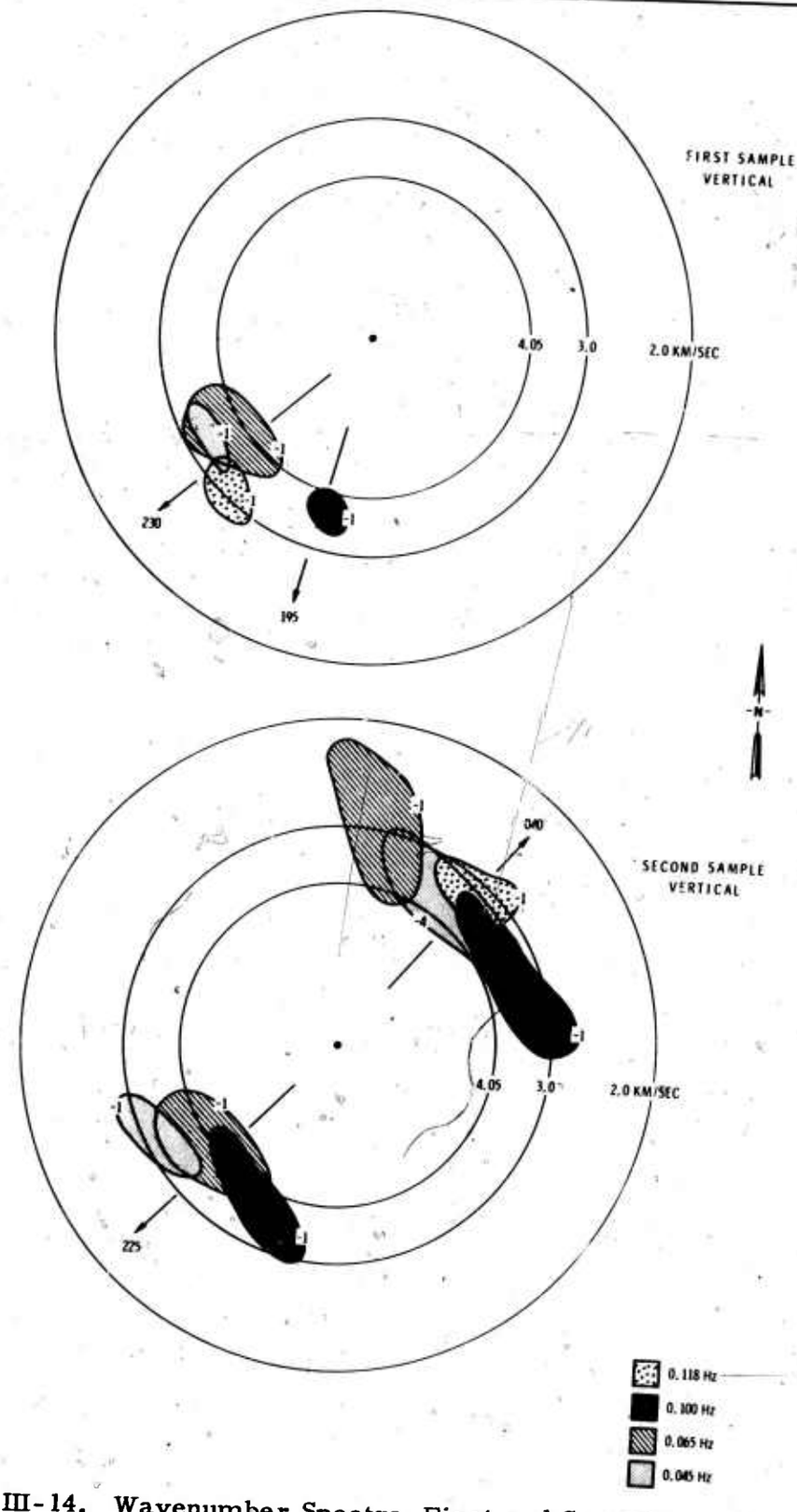

Figure III-14. Wavenumber Spectra-First and Second UBO Noise Samples

The wave height contour chart for the twelve hour period which includes this noise sample is presented in Figure III-15. The propagating energy shown on the f-k plots appears to be unrelated to wave activity.

The noise power ratios calculated as described earlier are presented for the vertical components of this noise sample in Figure III-16. A maximum in the noise rejection improvement for both the maximum likelihood and the beamsteer processors occurs at a frequency corresponding to the lower peak in the single channel power density spectra. The noise rejection improvement of the beamsteer processor over a single channel averages approximately 6.4 db. The average noise rejection improvement of the maximum likelihood processor is less than 2 db above this figure.

The coherence between the center vertical component and the other vertical components of the array for the first UBO noise sample is shown in Figure III-17. The region of most coherence is narrower and appears at a higher frequency than for the same set of components at TFO, in this case being centered in the same frequency region as the lower single channel power spectral density peak. The degree of coherence is less in this case, also.

D. SECOND UBO NOISE SAMPLE – 1800 Z, 27 July 1969

The single channel power density spectra computed from this noise sample are shown in Figure III-18. These spectra are almost identical to those of the first UBO noise sample both in shape and in level, and the same comments apply. The RMS noise levels for this noise sample are given in

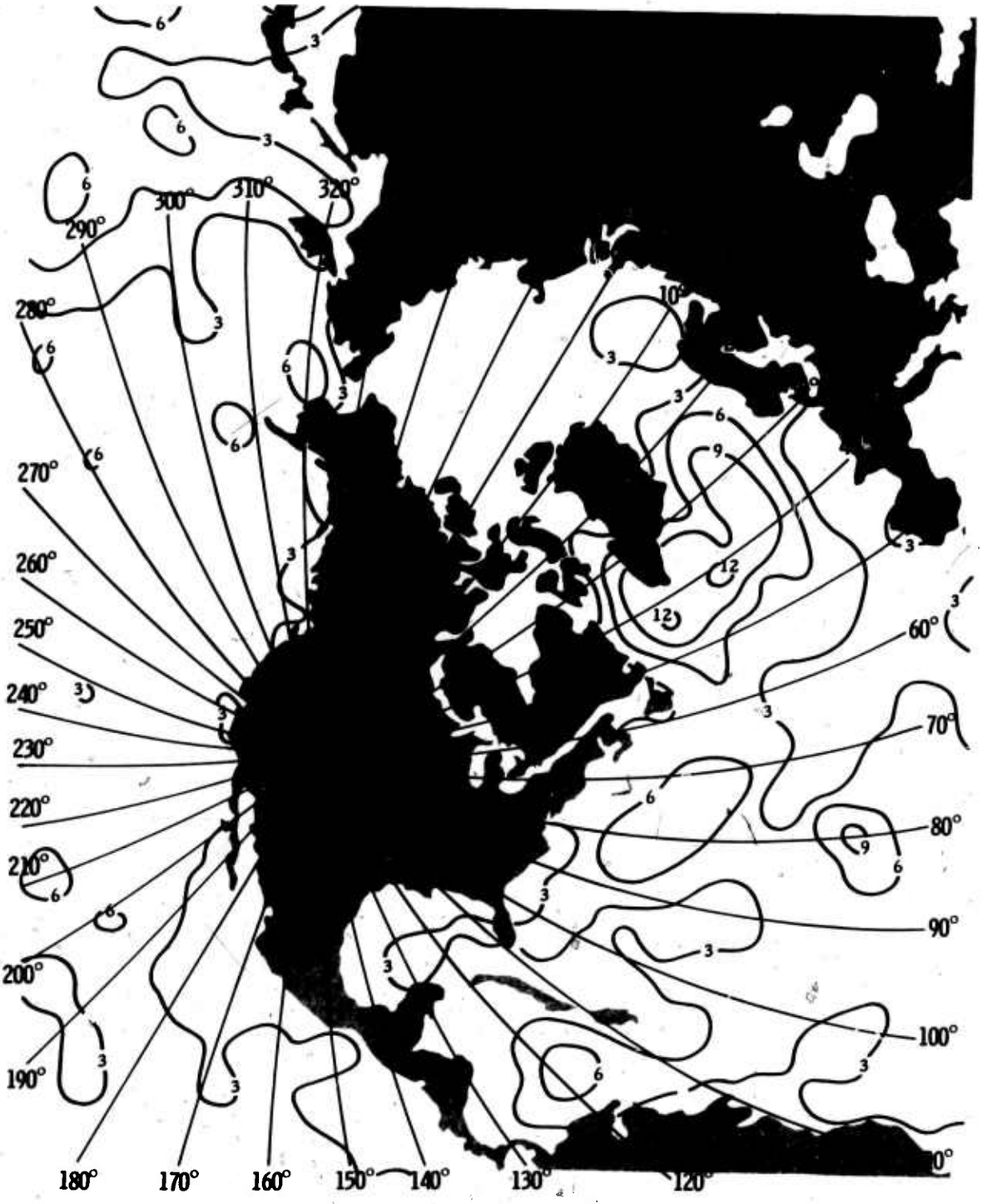

Figure III-15. Waveheight Chart at 1200 Z, 27 July 1969

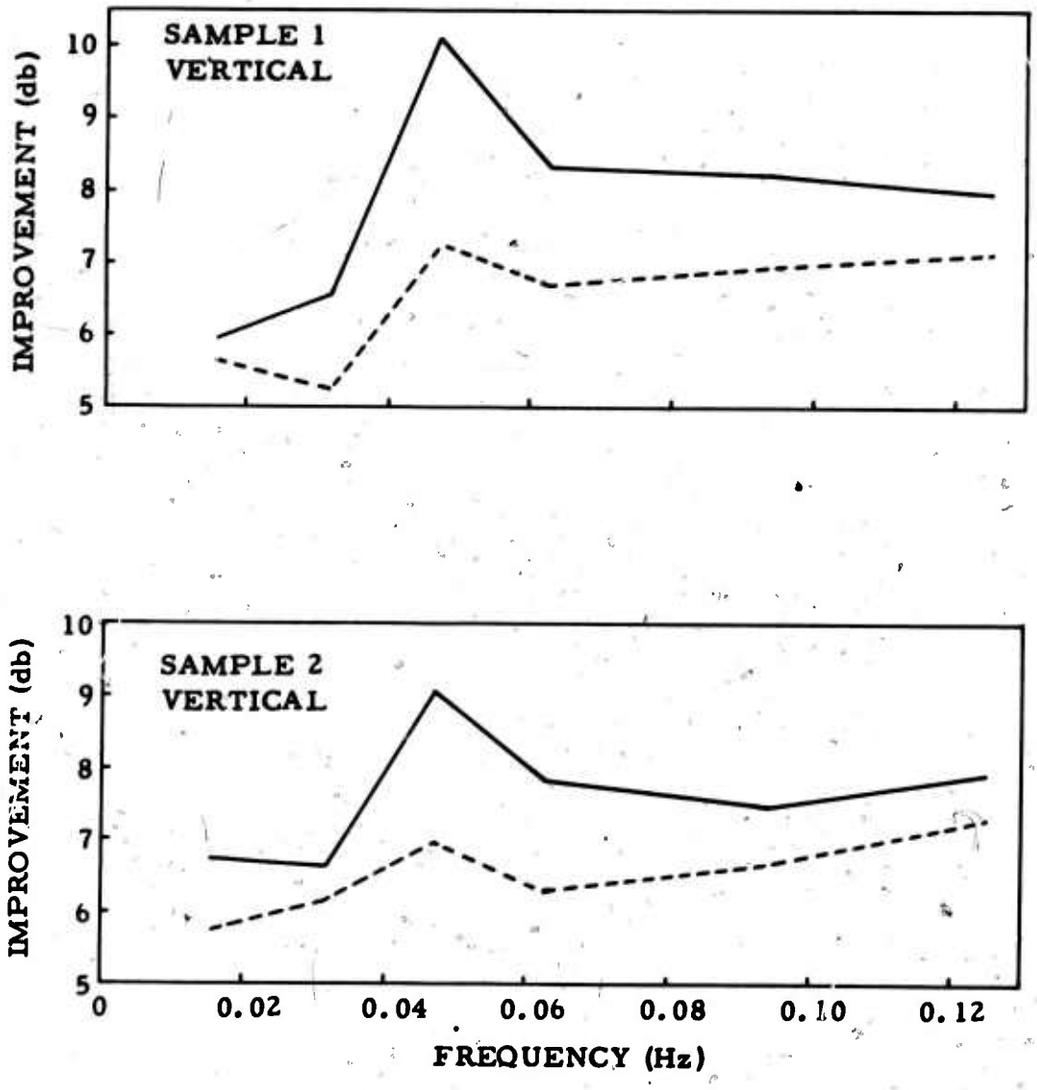

Figure III-16. Noise Rejection Improvement vs Frequency-First and Second UBO Noise Samples

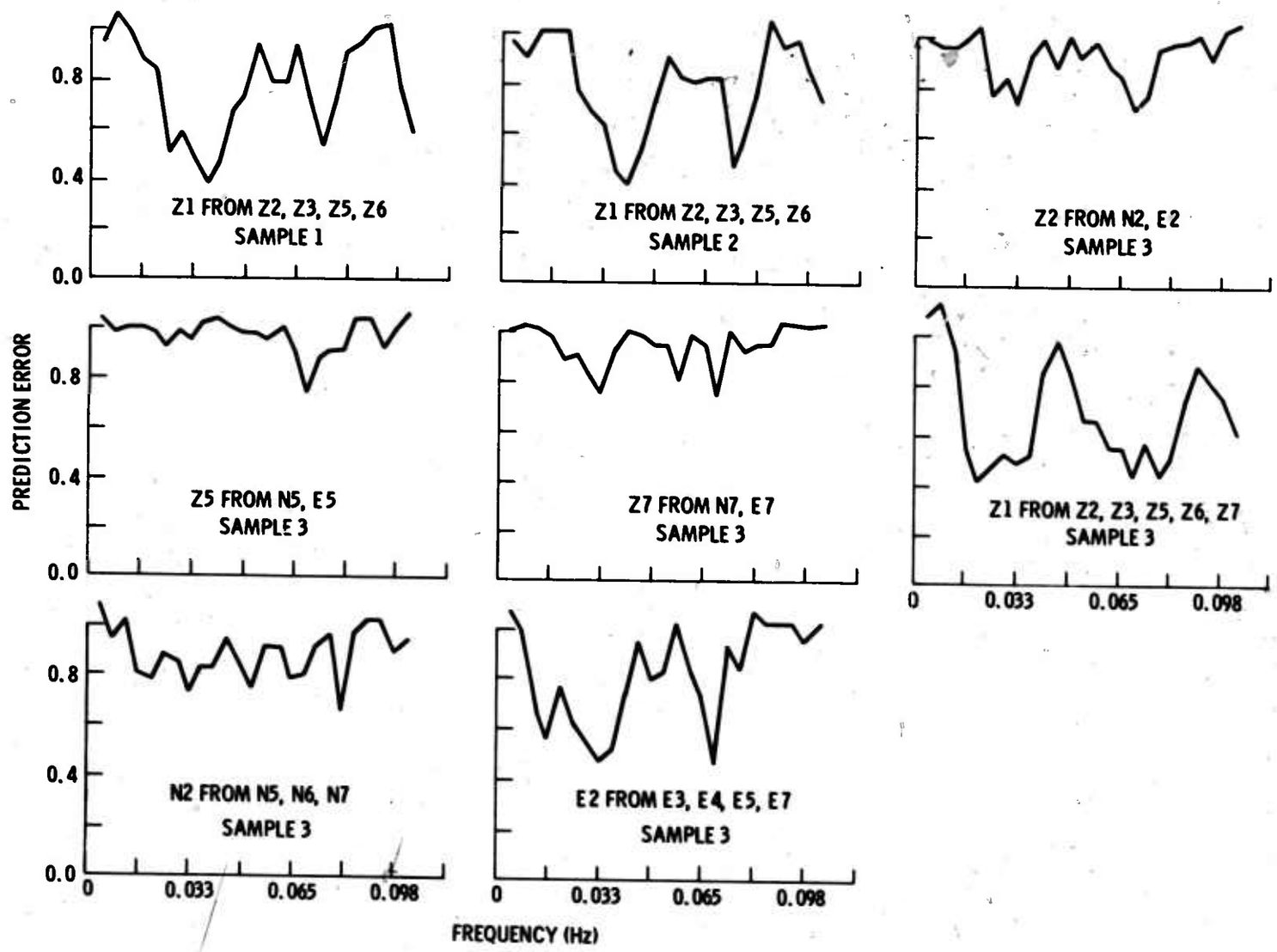

Figure III-17. Multiple Coherences-UBO Noise Samples

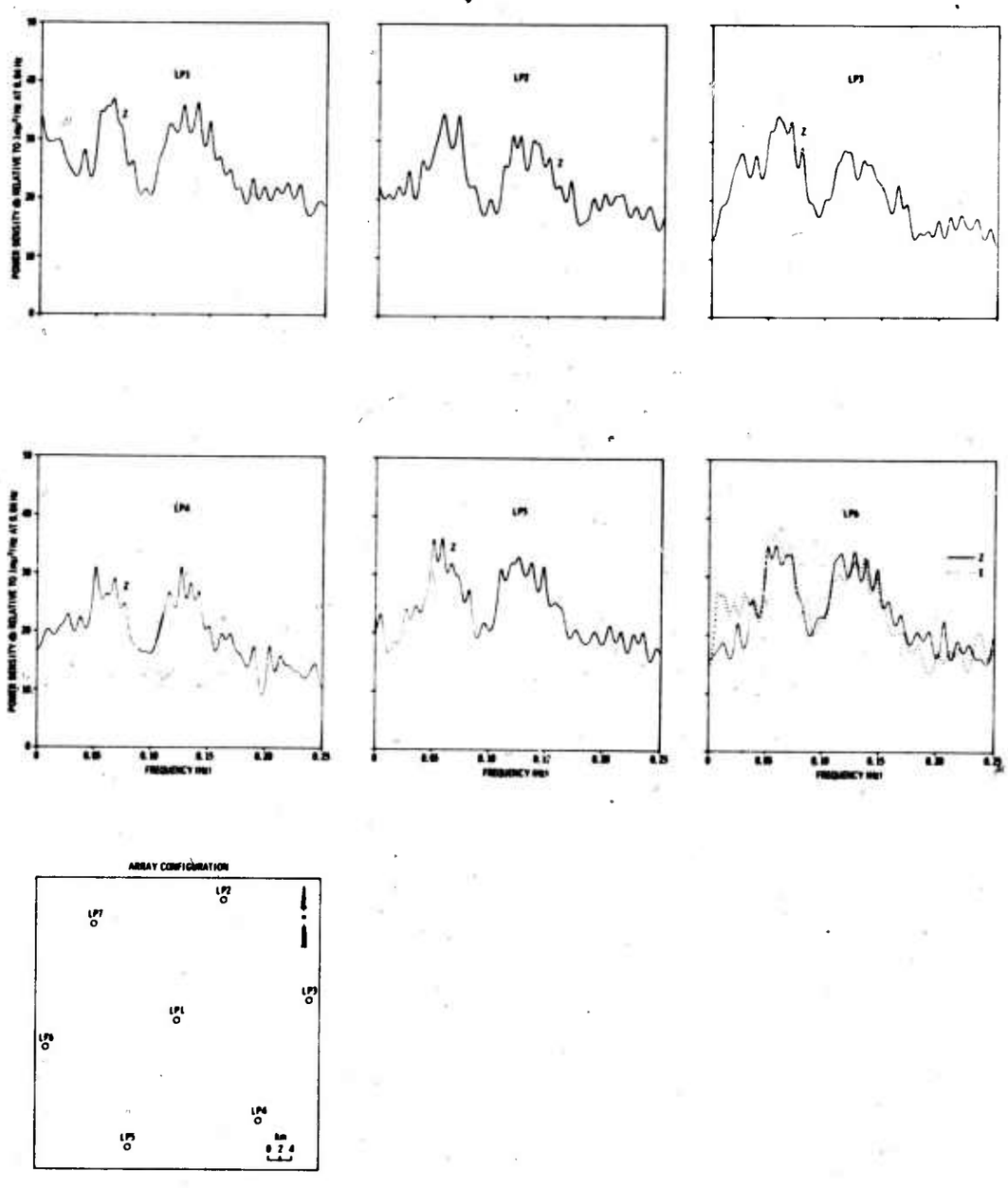

Figure III-18. Single Channel Power Density Spectra-Second UBO Noise Sample

Table III-2. There is less than 2 millimicrons difference in ground motion at any one site between this and the first noise sample.

The condensed f-k spectra of the vertical components in the second UBO noise sample are shown in Figure III-14. The significant peaks of propagating energy occur in the fundamental Rayleigh mode velocity range; the most significant peaks are in the northeast and southwest quadrants in azimuth ranges centered near 040° and 225°. The wave height contour chart appropriate to this noise sample, Figure III-15, shows no significant wave activity along the coasts.

The noise power ratios are presented for the vertical components of this noise sample in Figure III-16. Again, the maximum likelihood processor does less than 2 db better than the 6.5 db average improvement of the beamsteer processor over the frequency range.

The coherence between the center vertical component and the other vertical components is shown in Figure III-17. Again, the results are similar to those of the first UBO noise sample and the same comments apply.

E. THIRD UBO NOISE SAMPLE – 1227 Z, 30 JULY 1969

The single channel power density spectra for the third UBO noise sample are shown in Figure III-19. These spectra show the same higher spectral levels on the horizontal components below 0.05 Hz when compared to the vertical component at the same site. The two broad spectral peaks appear to be shifted downward in frequency in this noise sample, covering bands from 0.04 to 0.06 Hz and 0.10 to 0.13 Hz.

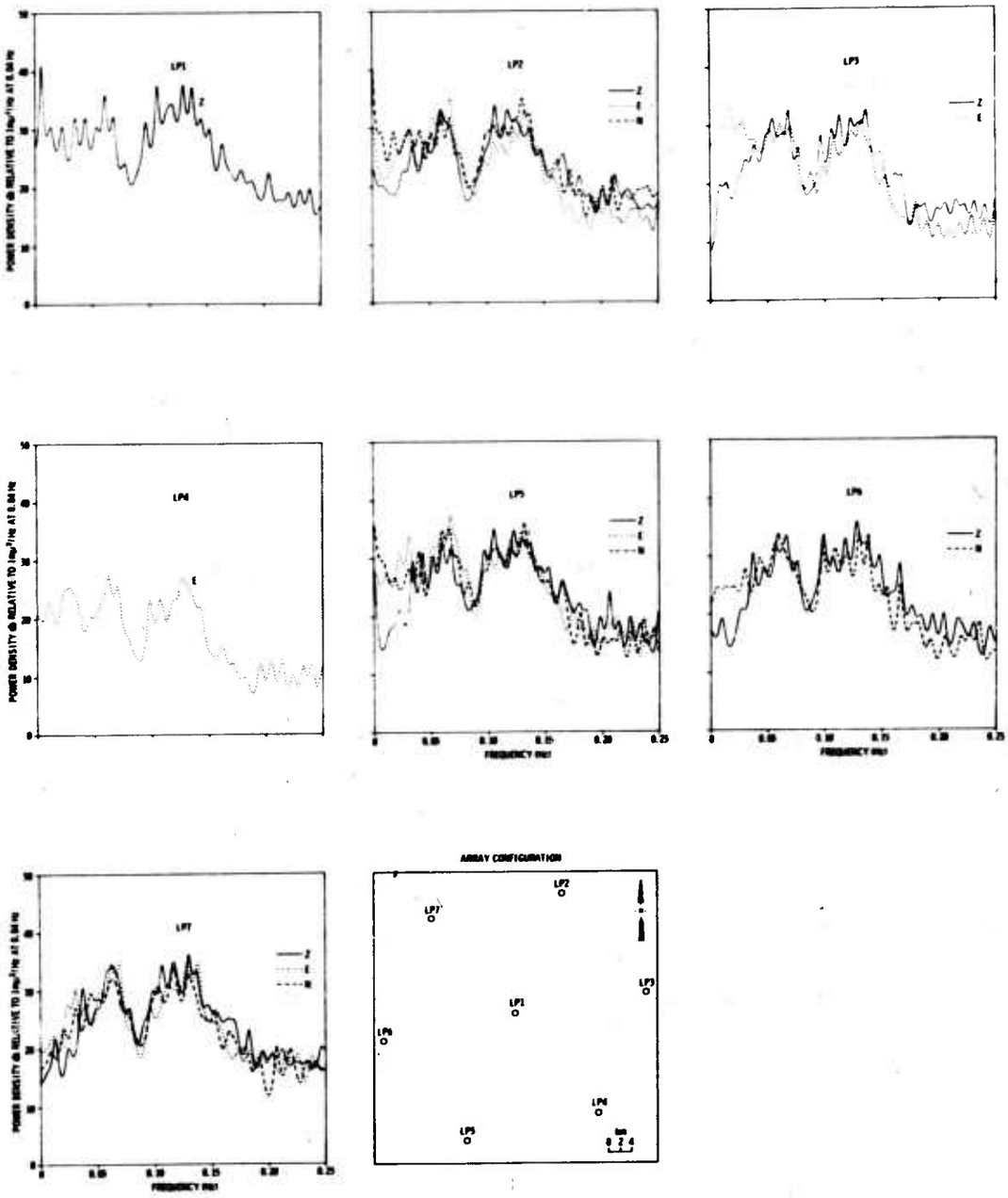

Figure III-19. Single Channel Power Density Spectra-Third UBO Noise Sample

RMS noise levels for this noise sample are given in Table III-2. These levels are very close to those of the two preceding UBO noise samples. The maximum variation in the level of any component among the three noise samples is less than 3.6 millimicrons.

The condensed f-k spectra for the three sets of components are shown in Figure III-20. While most of the propagating noise peaks appear to occur in the Rayleigh velocity range, some of the peaks at 0.094 Hz and 0.125 Hz occur at velocities greater than 15 km/sec, indicating the presence of P-wave energy at these frequencies. The dominant azimuths in this noise sample are those near 195°, 240°, and 320°.

The wave height chart for the twelve hour period in which this noise sample occurs is shown in Figure III-21. There appears to be no explanation of the propagating energy in this noise sample in terms of wave activity along the coasts.

The noise power ratios for the three sets of sensors are shown in Figure III-22. Again, there is less than 2 db average difference between the noise rejection capabilities of the maximum likelihood and beamsteer processors.

The multiple coherences computed for this noise sample are shown in Figure III-17. In contrast to the TFO data, there is very little coherence in this data between the vertical component and the horizontal components at the same location. The coherence between the center vertical component and the other vertical components shows two regions of relatively high coherence corresponding roughly to the two single-channel power spectral

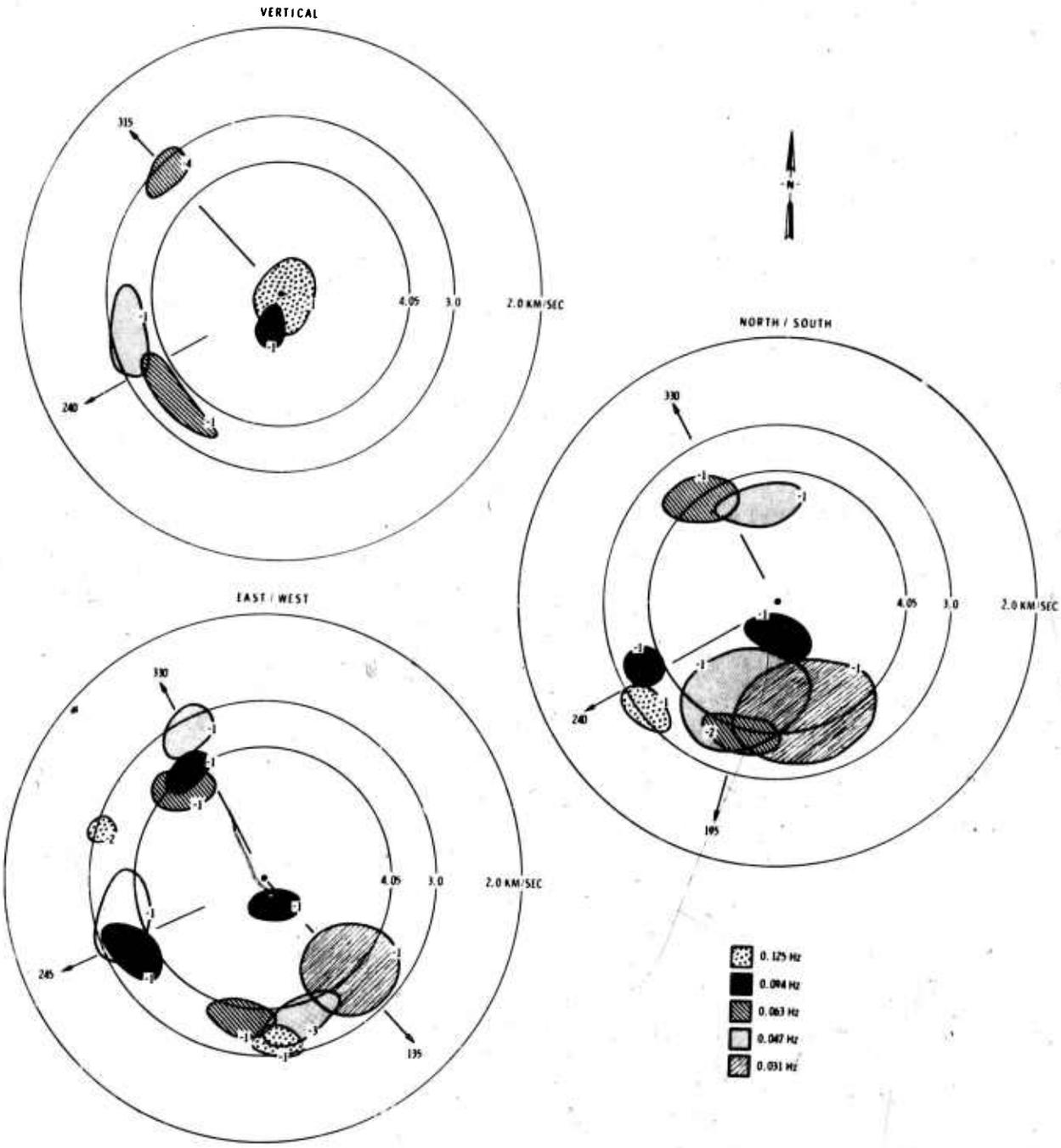

Figure III-20. Wavenumber Spectra-Third UBO Noise Sample

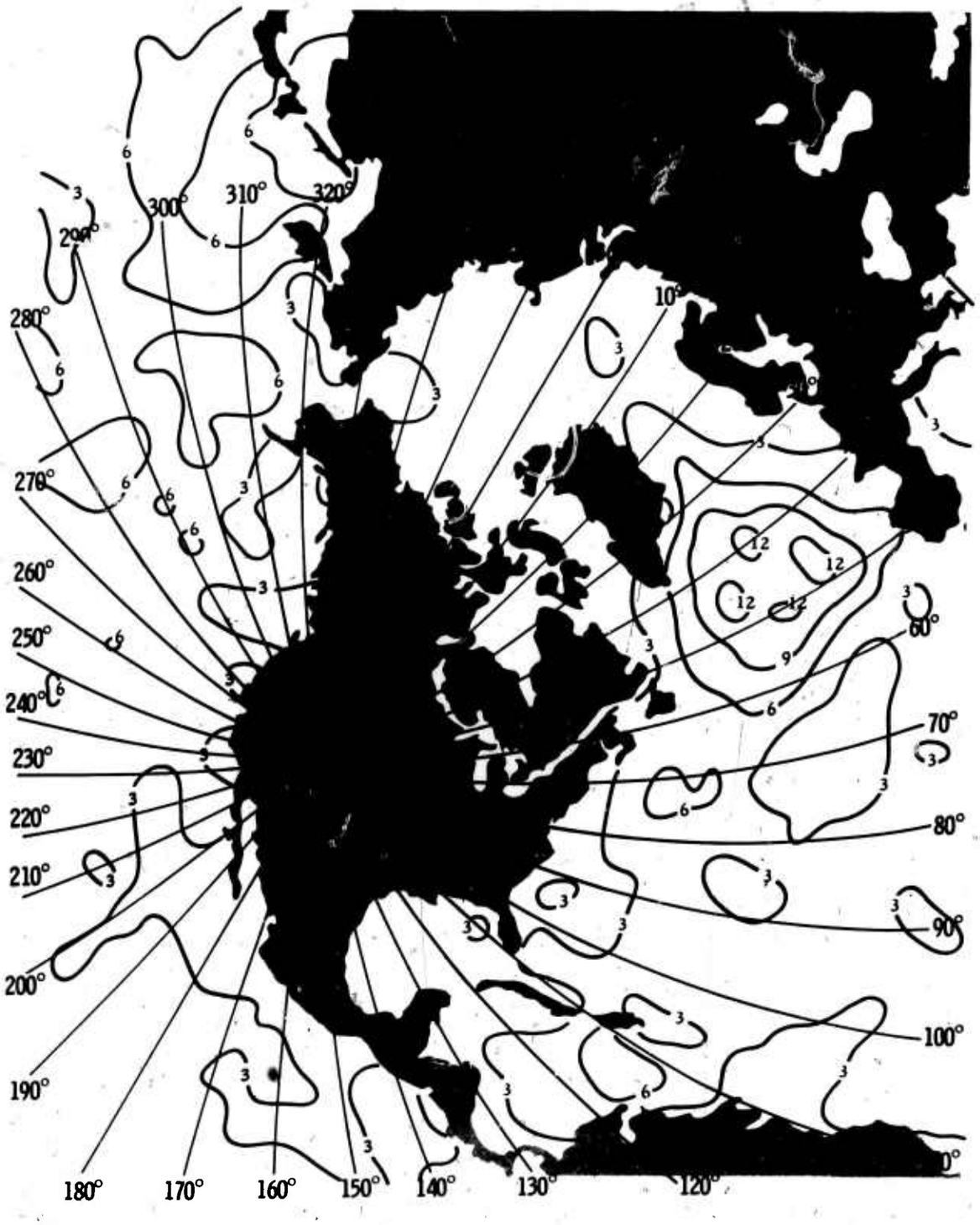

Figure III-21. Waveheight Contour Chart at 1200 Z, 30 July 1969

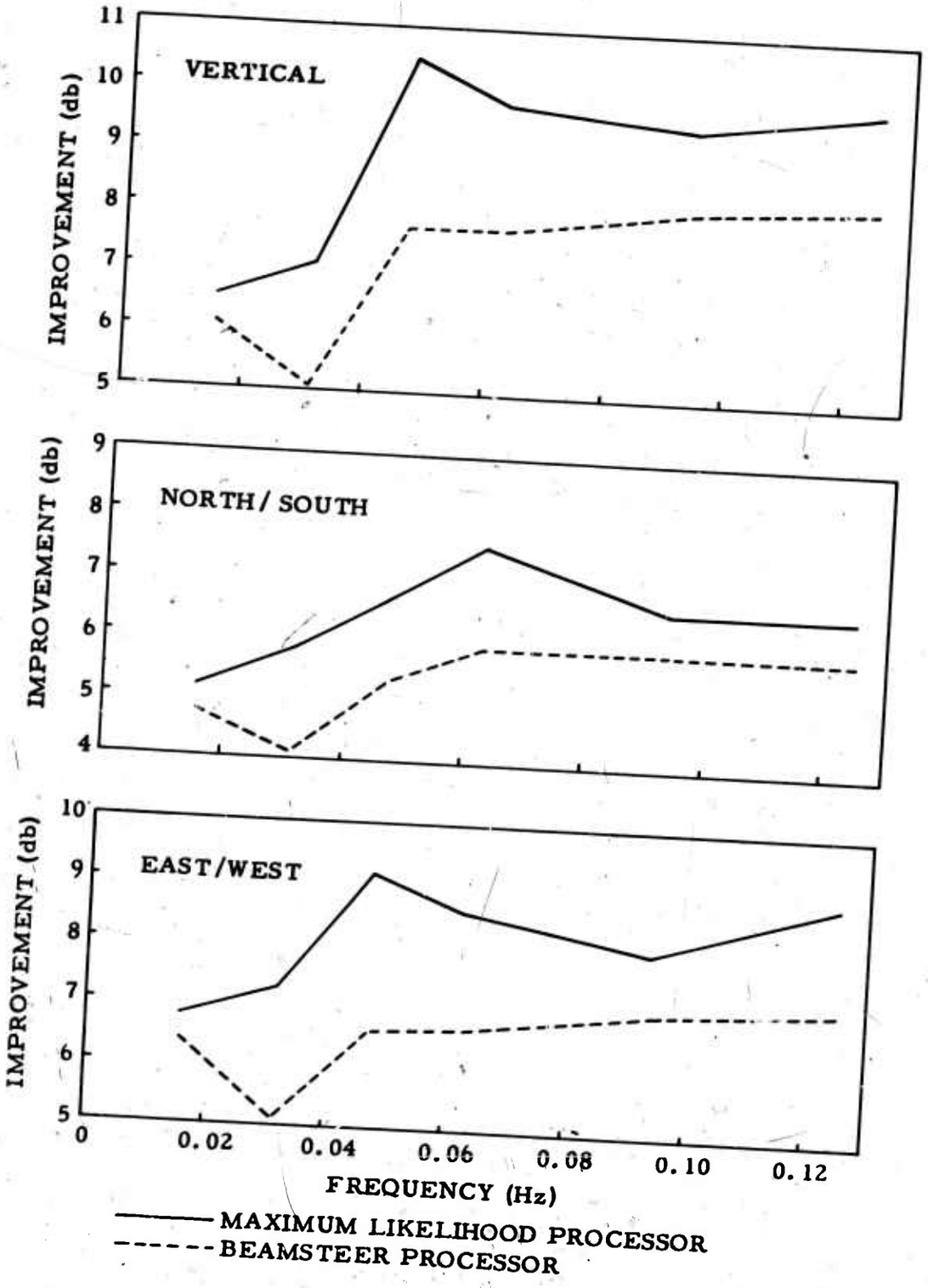

Figure III-22. Noise Rejection Improvement vs Frequency-Third UBO Noise Sample

peaks, as in the first two UBO samples. However, the regions are slightly wider and occur at slightly lower frequencies in this noise sample. Since the data from the horizontal components of the center (LP1) seismometer were not useable, the coherence between each horizontal component at LP2 and the other like horizontal components was computed. There is less coherence than expected between the north-south component at LP2 and the other north-south components. The plot of the coherence between the LP2 east-west component and the other east-west components has a more normal appearance, showing the same general characteristics as the equivalent vertical coherence plots for the 3 UBO noise samples.

SECTION IV

LOW VELOCITY PEAKS IN THE LOW FREQUENCY f-k SPECTRA AT TFO

Examination of the f-k spectra of the TFO noise samples showed evidence of an unusual low velocity spectral peak. The peak occurred only in the 0.0163 Hz frequency-wavenumber plots for the east - west components of the first noise samples and the north - south components of the second noise sample. The energy appeared to propagate from the southwest at a velocity near the edge velocity of the plots, two km/sec.

In order to determine whether this peak was an alias of a still lower velocity spectral peak, the f-k spectra were re-computed using a 0.25 km/sec edge velocity. These f-k spectra are shown in Figures IV-1 and IV-2. The peak from the southwest at approximately 2 km/sec is an alias of a peak which in both plots appears at an azimuth of approximately 80° and a velocity of approximately 0.41 km/sec, or 1350 ft/sec. This is somewhat higher than the velocity of sound in air, 1100 ft/sec. There appears to be no obvious explanation of this peak in terms of either ordinary acoustic or seismic wave velocities, but the peak is suspiciously close to acoustic velocities.

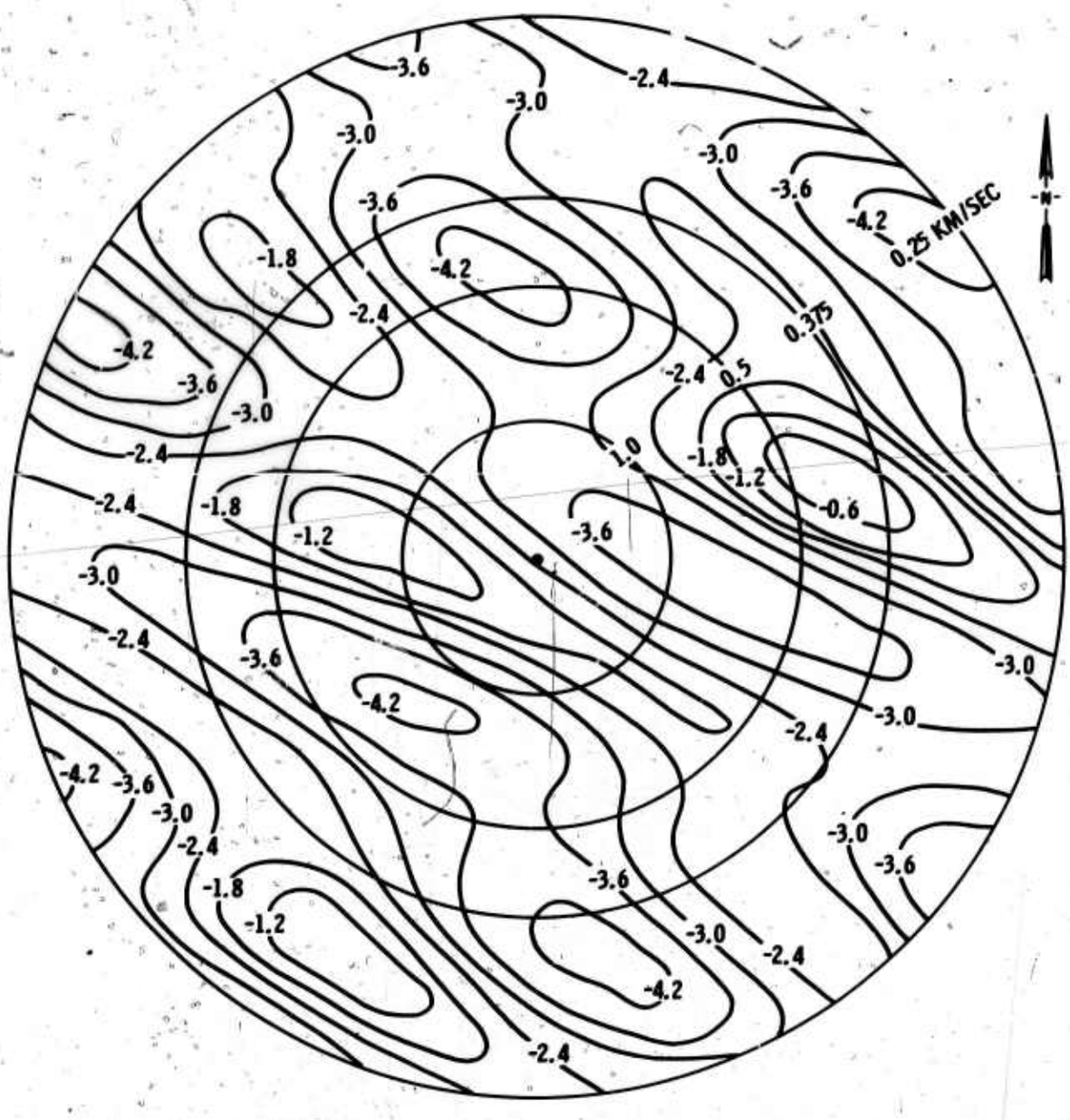

Figure IV-1. TFO Wavenumber Spectrum at 0.0163 Hz

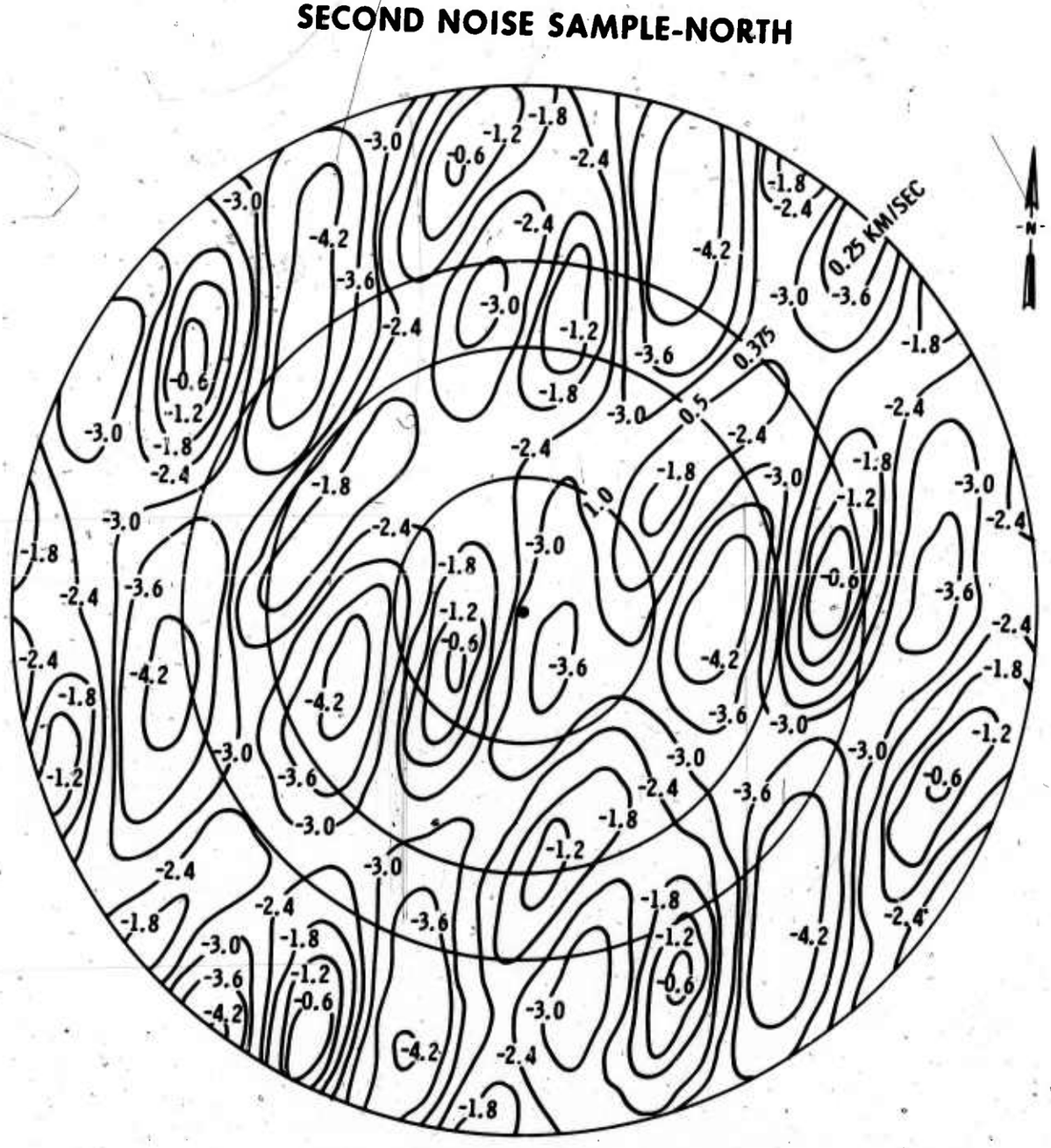

Figure IV-2. TFO Wavenumber Spectrum at 0.0163 Hz

SECTION V

CONCLUSION-COMPARISON OF THE LASA, TFO, AND UBO NOISE FIELDS

The conclusions reached through the foregoing analysis are presented here principally in terms of a comparison with results obtained earlier through the analysis of LASA long-period noise samples. To facilitate the comparison certain of the figures from the Large Array Signal and Noise Analysis Final Report[4] are reproduced here.

The single-channel power density spectra of seven winter noise samples and five summer noise samples recorded in 1966 - 1967 at the center LP seismometer (AO) of the LASA array are shown in Figures V-1 and V-2. The spectra at TFO, UBO, and LASA exhibit an overall similarity. The most apparent similarities among the spectra from the three arrays are these:

- Variations in the noise level on a given channel at different times are most pronounced below 0.05 Hz.
- In general, below 0.05 Hz the horizontal components are several db noisier than the vertical component at the same site
- The spectra at each array exhibit two peaks, one lying in the 0.05 - 0.07 Hz region and the other in the 0.11 - 0.14 Hz region

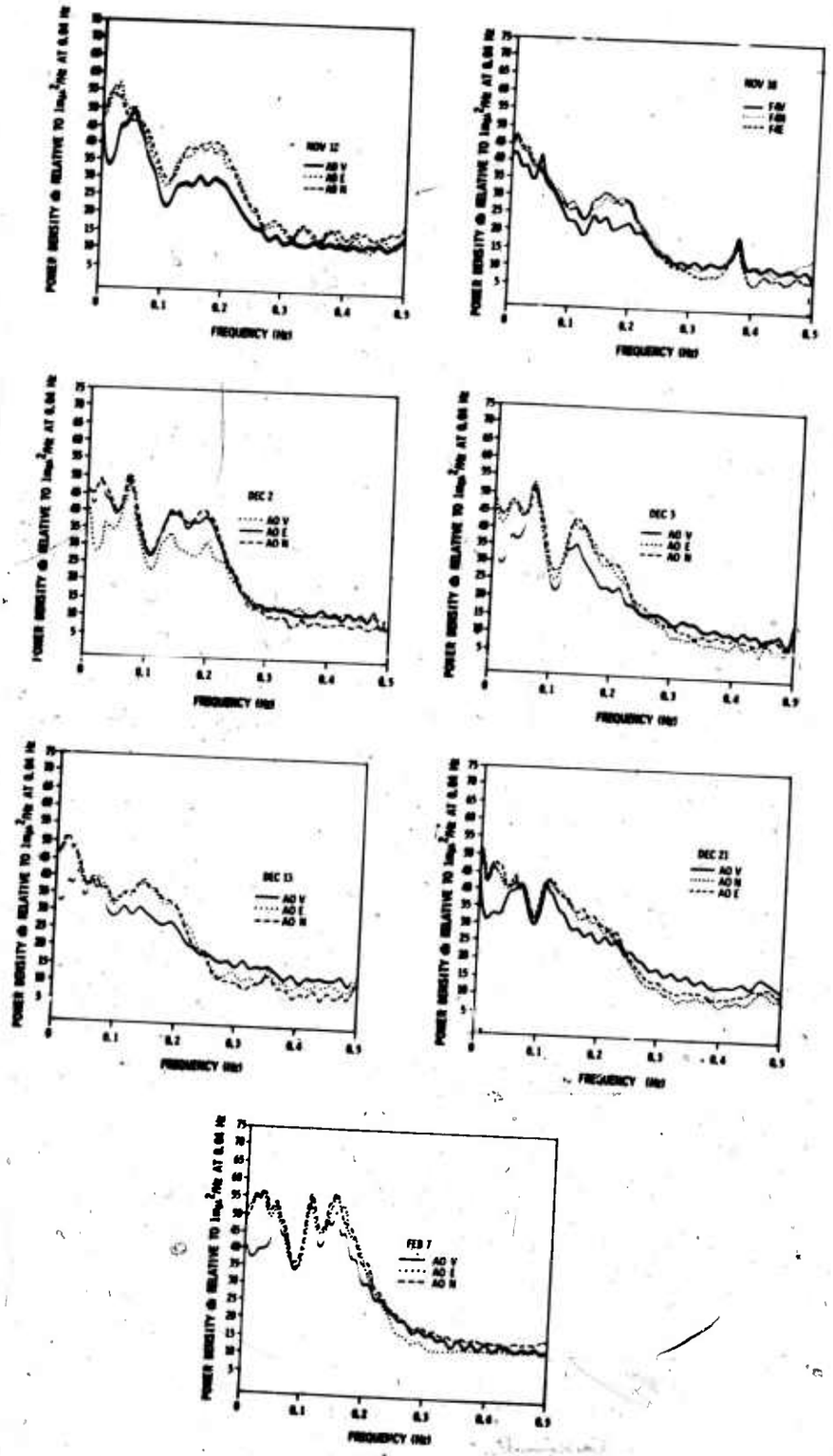

Figure V-1. Single Channel Power Density Spectra for Seven LASA Winter Noise Samples

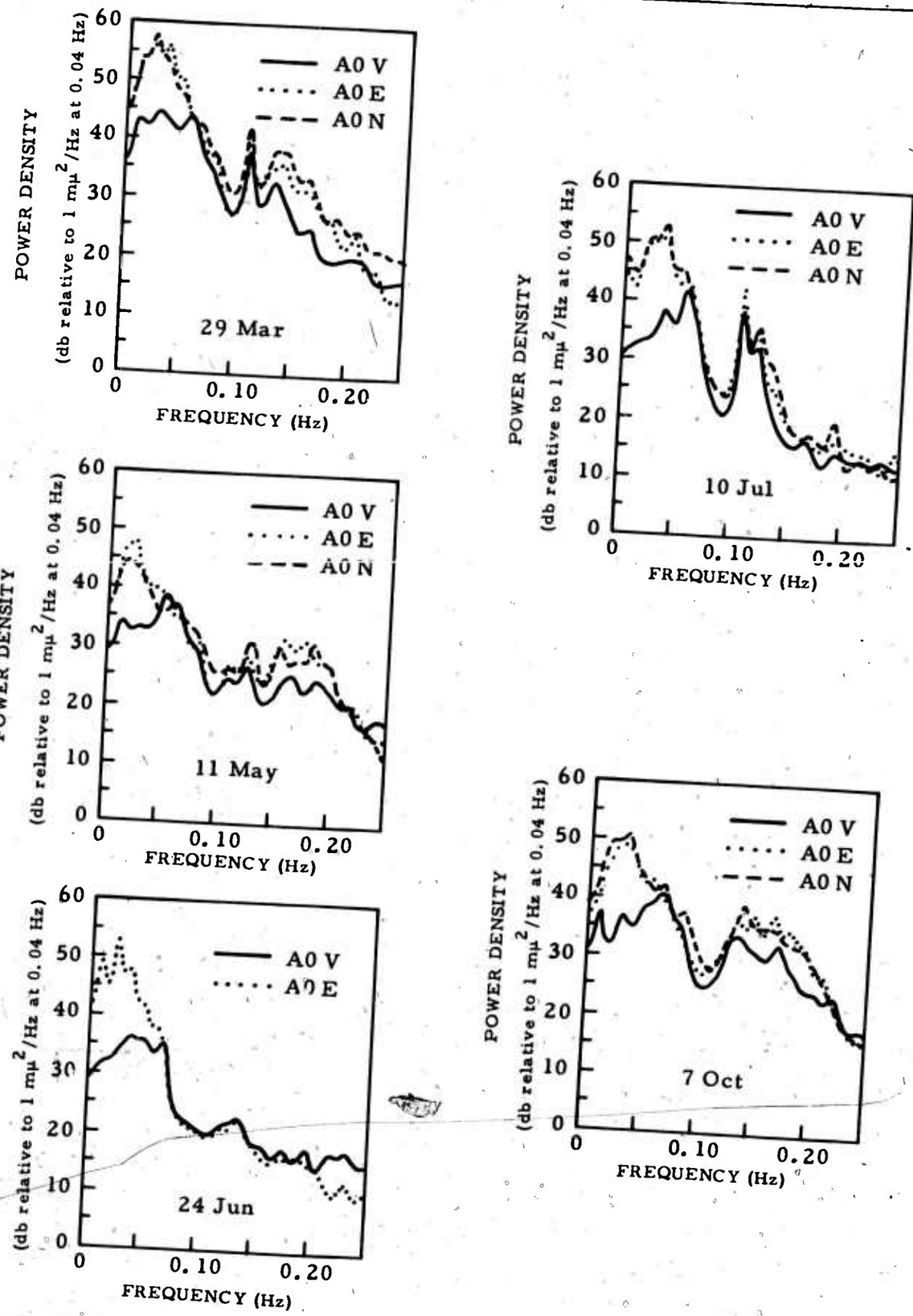

Figure V-2. Single Channel Power Density Spectra for Five LASA Summer Noise Samples

The main differences in the spectra are the following:

- The TFO spectra are all very similar in shape, as are the UBO spectra; the LASA spectra for different components and times vary more substantially
- The upper spectral peak ($\approx$ 0.11 - 0.14 Hz) is broader in frequency and more variable in level at LASA than at TFO or UBO
- The LASA summer noise spectral levels are for most of the examples more than 5 db above the UBO spectral levels
- In the 0.05 - 0.07 Hz region, the LASA winter noise spectral levels range up to 10 db higher than those of the TFO data.

Multiple coherences determined for various sets of components at LASA are shown in Figures V-3 through V-6. These show some of the same features noted in the coherences computed from the TFO and UBO data. For example, a vertical-horizontal coherence peak generally occurs in the 0.05-0.07 Hz region. Also, the vertical coherences in the first two UBO noise samples are like those at LASA in that there is little coherence below 0.05 Hz. In the noise samples studied, the vertical coherence does not fall off as rapidly below 0.05 Hz at TFO as at LASA. In general, both the vertical and horizontal coherences are higher at LASA than at either TFO or UBO.

The results of the analysis of the f-k spectra for TFO and UBO show that these exhibit most of the characteristics of the LASA f-k spectra:

- Fundamental Rayleigh mode energy appears to dominate the propagating component

- Some evidence of a higher frequency P-wave component occurs in certain quiet summer noise samples

- Winter f-k noise peaks can often be related to coastal wave activity; this relationship is much less prominent in summer noise f-k spectra

Beamsteer processing of the TFO and UBO data resulted in an average signal-to-noise ratio improvement of approximately 6.5 db over the frequency range of most interest. (<.1 Hz). This figure is very close to the $\sqrt{N}$ improvement expected for the N channels in use (from four to six channels in these examples). Maximum likelihood MCF array processing resulted in little more than 2 db average improvement above the 6.5 db achieved by the beamsteer processor.

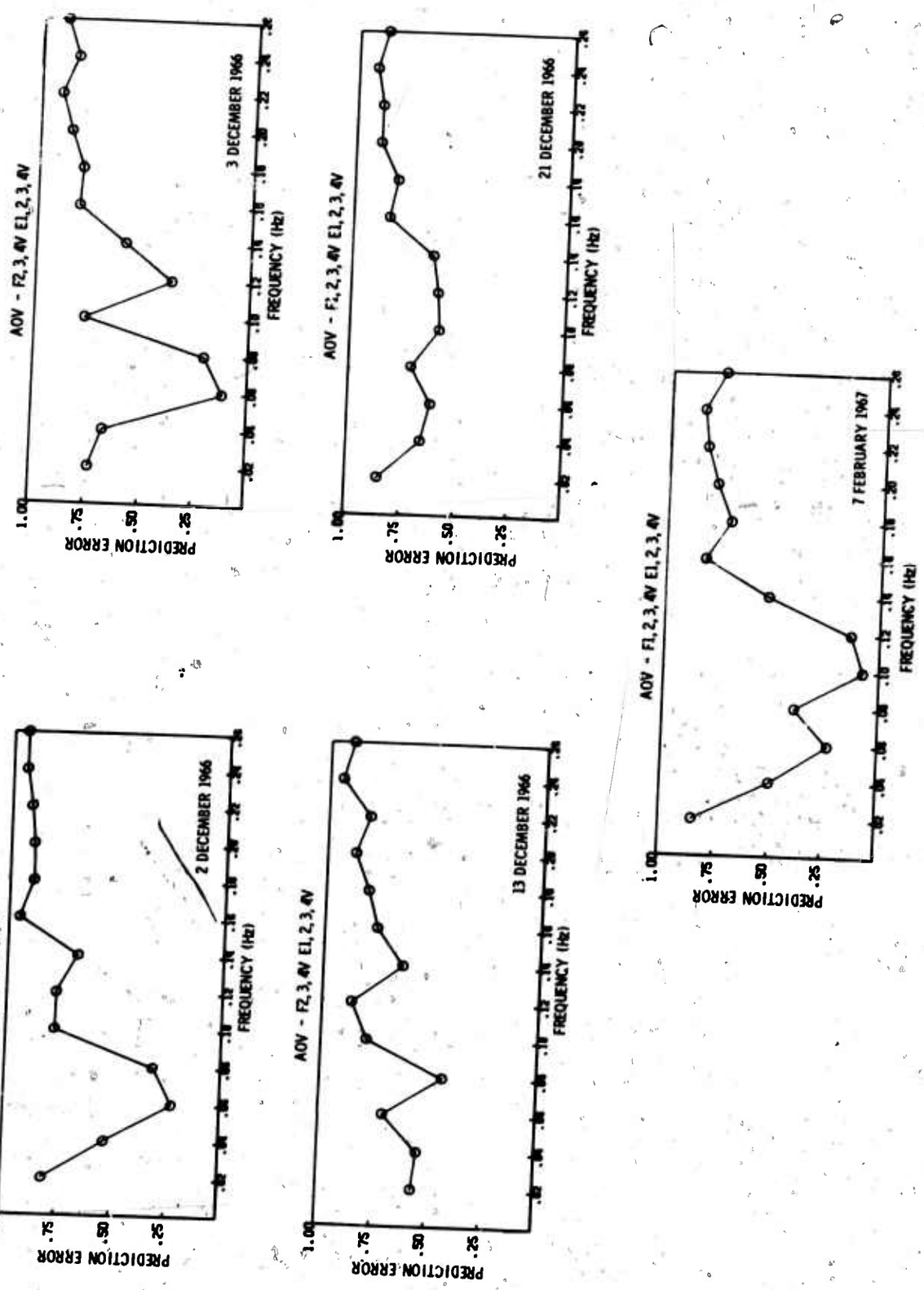

Figure V-3. Vertical Coherences of Five LASA Winter Noise Samples

Figure V-3. Vertical Coherences of Five Winter Noise Samples

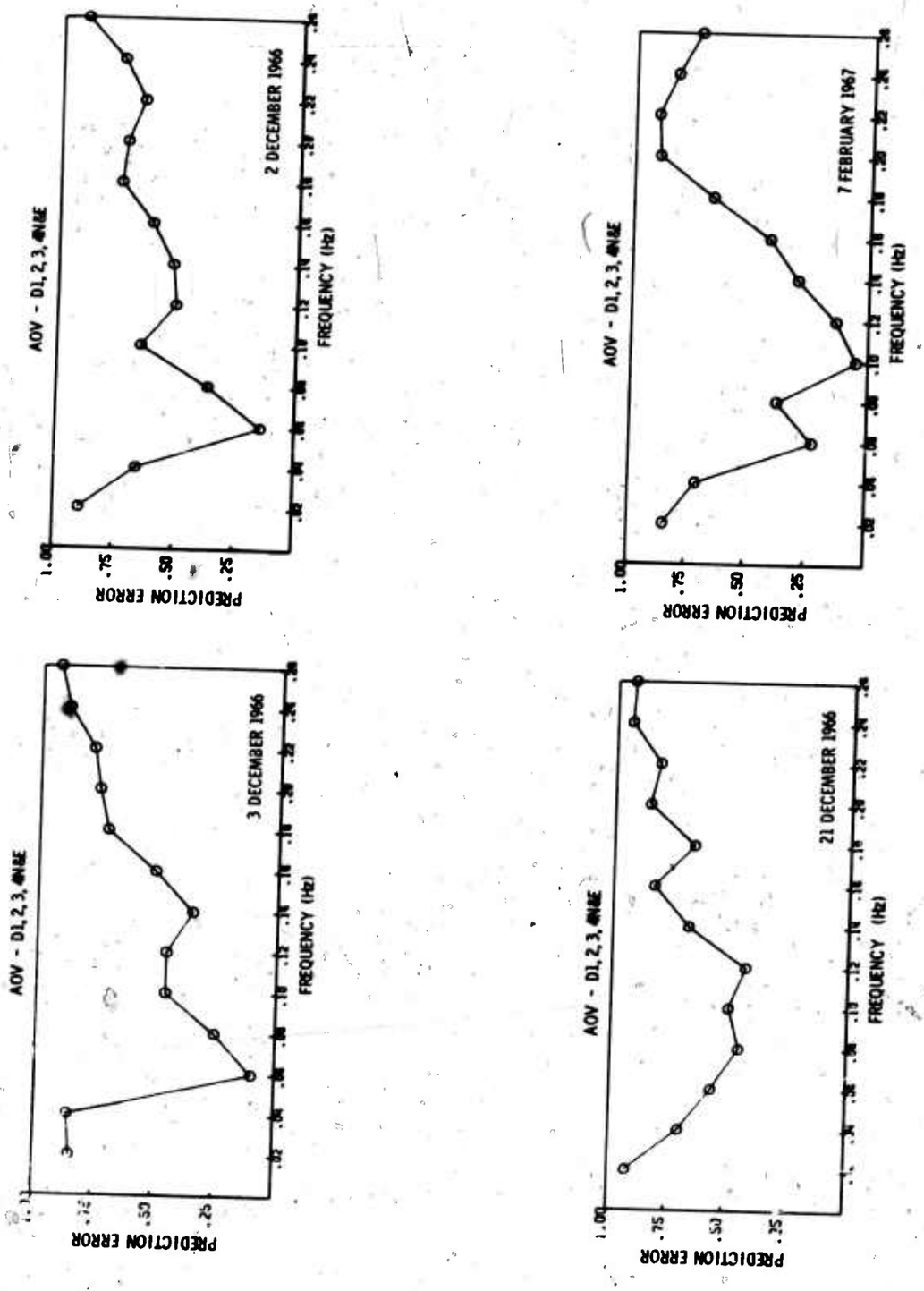

Figure V-4. Vertical-Horizontal Coherences of Four Winter Noise Samples

Figure V-4. Vertical-Horizontal Coherences of Four LASA Winter Noise Samples

24 Jun 1967

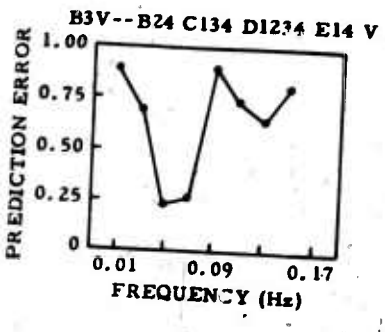

29 Mar 1967

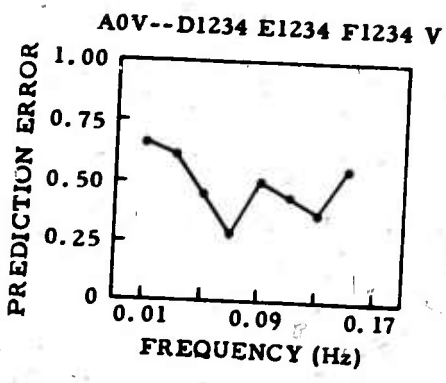

11 May 1967

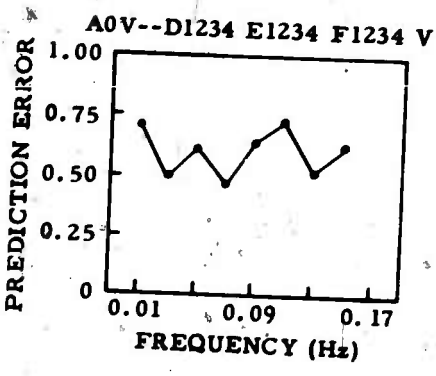

10 Jul 1967

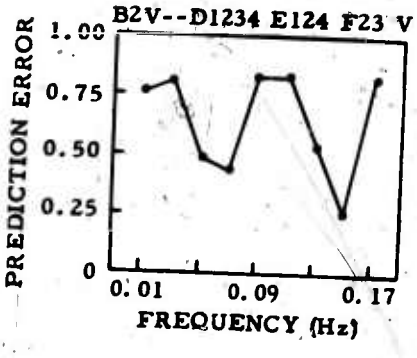

7 Oct 1967

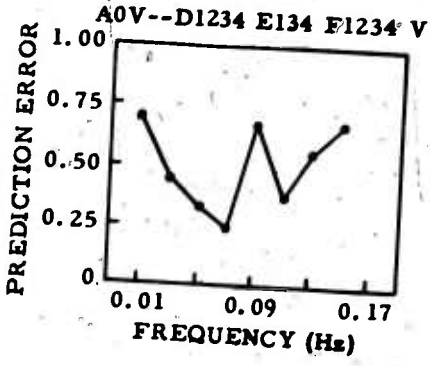

Figure V-5. Vertical Coherences of Five LASA Summer Noise Samples

24 Jun 1967

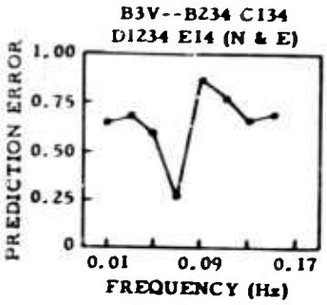

29 Mar 1967

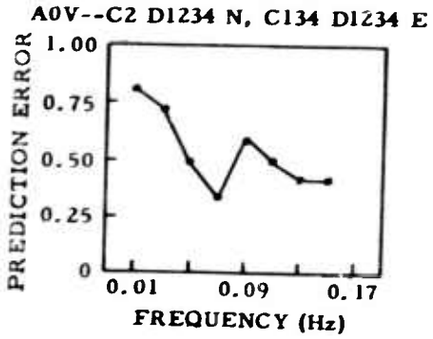

11 May 1967

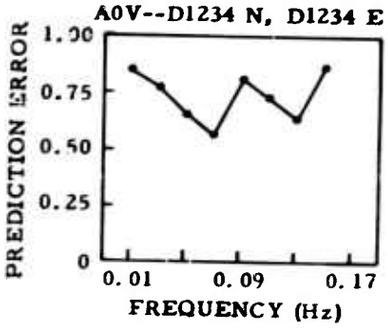

10 Jul 1967

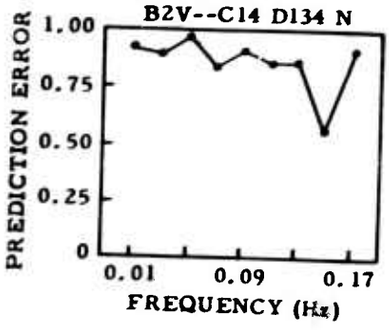

7 Oct 1967

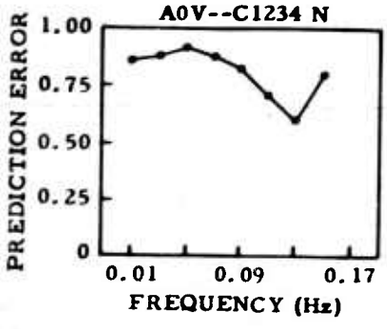

Figure V-6. Vertical-Horizontal Coherences of Five LASA Summer Noise Samples

SECTION VI

REFERENCES

1. Burg, J.P., Proceeding of NATO Conference on Signal Processing with Emphasis on Underwater Acoustics, 1968: Maximum Entropy Spectral Analysis.

2. Blackman and Tukey, 1959: The Measurement of Power Spectra, Dover Publications, Inc., New York.

3. Burg, J.P., Texas Instruments Incorporated, 1967: Statistics Governing the Design and Performance of Noise-Prediction Filters, Contract F33657-67-C-0708-P001.

4. Texas Instruments Incorporated, 1968: Large-Array Signal and Noise Analysis, Final Report, Contract AF33(657)-16678, 6 Dec.

5. Texas Instruments Incorporated, 1960: Seismometer Array and Data Processing System Phase I, Final Report, Contract AF33(600)-41840, p 110.

UNCLASSIFIED
Security Classification

DOCUMENT CONTROL DATA – R & D
(Security classification of title, body of abstract and indexing annotation must be entered when the overall report is classified)

1. ORIGINATING ACTIVITY (Corporate author)
Texas Instruments Incorporated
Services Group
P. O. Box 5621, Dallas, Texas 75222

2a. REPORT SECURITY CLASSIFICATION
Unclassified

2b. GROUP
—

3. REPORT TITLE
TFO AND UBO LONG-PERIOD ARRAY DATA ANALYSIS
SEISMIC ARRAY PROCESSING TECHNIQUES TECH. RPT. NO. 8

4. DESCRIPTIVE NOTES (Type of report and inclusive dates)
Technical

5. AUTHOR(S) (First name, middle initial, last name)
Gary D. McNeely

6. REPORT DATE	7a. TOTAL NO. OF PAGES	7b. NO. OF REFS
12 August 1970	53	4

8a. CONTRACT OR GRANT NO.	9a. ORIGINATOR'S REPORT NUMBER(S)
F33657-70-C-0100	—
b. PROJECT NO. VELA/T/0701/B/ASD	
c.	9b. OTHER REPORT NO(S) (Any other numbers that may be assigned this report)
d.	—

10. DISTRIBUTION STATEMENT
This document is subject to special export controls and each transmittal to foreign governments or foreign nationals may be made only with prior approval of Chief, AFTAC.

11. SUPPLEMENTARY NOTES	12. SPONSORING MILITARY ACTIVITY
ARPA Order No. 624	Advanced Research Projects Agency Department of Defense The Pentagon, Washington, D. C. 20301

13. ABSTRACT

Results of the analysis of two long-period noise samples from Tonto Forest Seismological Observatory (TFO) and three from Uinta Basin Seismological Observatory (UBO) are presented. Analysis methods include single channel power density spectra, determination of multichannel coherences, and computation of two-dimensional frequency-wavenumber spectra. Results are compared to results obtained earlier from the Montana Large Aperture Seismic Array; the noise fields at the three sites are found to be generally similar. Comparison of array processing methods for the UBO and TFO data indicate that little more than 2 db noise suppression improvement above the 6-7 db obtainable by beamsteer processing can be expected from multichannel filter processing. There is some evidence of acoustically coupled low-frequency propagating noise in the TFO data.

DD FORM 1 NOV 65 1473

UNCLASSIFIED
Security Classification

14. KEY WORDS	LINK A ROLE	LINK A WT	LINK B ROLE	LINK B WT	LINK C ROLE	LINK C WT
Tonto Forest Seismological Observatory						
Uinta Basin Seismological Observatory						
Long-Period Noise						
Spectral Analysis						
Seismic Noise Sources						